

On the Ring-Opening of the
Pyrido-[1,2a]-Pyrimidinium Cations

Michael Peter Jansen

A Thesis
in
The Department
of
Chemistry

Presented in Partial Fulfillment of the Requirements
for the degree of Master of Science, at
Concordia University
Montréal, Québec, Canada

June 1984

© Michael Peter Jansen, 1984

ABSTRACT

On the Ring-Opening of the Pyrido-[1,2a]-Pyrimidinium Cations

Michael P. Jansen

The kinetics of the reversible ring-opening of the pyrido-[1,2a]-pyrimidinium cation (PP+) to 2-(2-pyridyl-amino)-acrolein (PA) were studied in aqueous solution, pH 0 - 14 (at 25°C, I = 1) using stopped-flow UV spectrophotometry. Several substituted derivatives were also prepared and examined. Various dynamic and static NMR studies were carried out.

The protonated pseudobase (PBH+) of PP+ was found to exist in equilibrium with PP+ to the extent of ca. 5%. It was observed by both NMR and UV spectroscopies. The kinetic studies revealed two distinct equilibrations: $\text{PBH}^+ \rightleftharpoons \text{PA}$ ($\text{pK}_a = 4.62$) and $\text{PP}^+ \rightleftharpoons \text{PA}$ ($\text{pK}_a = 5.90$). Four distinct pathways exist on the pH-rate profiles for these equilibrations and are summarised as follows: Process (a) involves the base-catalysed ring-opening of PBH+ to PA, probably via its zwitterion (PBZ). Process (b) is a base-catalysed ring-opening of PP+ to

yield PA.

Process (c) is the acid-catalysed ring-closure of PA to give PBH+ as a transient intermediate. The mechanism of this conversion involves a change in rate-limiting step with increasing acidity, as evidenced by curved buffer plots obtained.

Process (d) is the acid-catalysed dehydration of the transient PBH+ (formed in process (c)) to give the stable cation PP+. This conversion was clearly observed in a series of dynamic NMR spectra.

This thesis is dedicated to my family, and to Diane.
Without their support and encouragement I would never
have been able to "cut the mustard".

Acknowledgements

I would like to express my sincere gratitude and appreciation to Professor Oswald S. Tee for his guidance, assistance and encouragement throughout the course of this work.

Thanks are also due to those many others whose contributions have been invaluable:

- Professor R.A. McClelland of the University of Toronto, for helpful discussions.
- Professor L.D. Colebrook, who gave freely of his time in helping me with the operation of the WP-80SY NMR spectrometer and the HP-1000 mini-computer, used to prepare this text.
- Mr. Michael Trani, for preliminary experiments carried out on this system.
- The Department of Chemistry, for financial support and the Graduate Studies Office for a Graduate Fellowship.
- Finally, I thank my fellow graduate students and the members of the Chemistry Department (Faculty, Technicians and Secretaries) for their help, friendship and support during my stay at Concordia.

Table of Contents

PART I - INTRODUCTION

	page
General Introduction	1
Synthesis of the Pyrido-[1,2a]-Pyrimidinium Cations	3
Tetrahedral Intermediates and Pseudobase Formation	7
General Acid/Base (Buffer) Catalysis	12
The Stopped-Flow Method	17

PART II - EXPERIMENTAL

Materials	20
Kinetic Solutions	24
Determination of the Apparent pK_a between PP+ and PA.	26
Kinetic Apparatus	26
Kinetic Procedure and Data Acquisition	28
Computer Programmes	31
Treatment of Kinetic Data	32

PART III - RESULTS AND DISCUSSION

Introduction	36
--------------	----

NMR Studies.	36
UV Spectra.	49
Kinetic Results	57

PART IV - SUMMARY	81
-------------------	----

PART V - REFERENCES	83
---------------------	----

PART IV - APPENDIX

Rate Constants for PP^+ , processes (a) through (d)	88
Rate Constants for the derivatives of PP^+	92
Rate Constants for Buffer Catalysis of $PA \rightleftharpoons PBH^+$	96

Index to Figures

No.	Content	page
1	Several derivatives of <u>PP+</u>	21
2	The stopped-flow data acquisition system	30
3	Dynamic NMR spectra of <u>PBH+</u> \rightarrow <u>PP+</u>	46
4	400 MHz. NMR of <u>PP+</u> in D_2O - DCl with 5% <u>PBH+</u> present	47
5	Static UV spectra of <u>PP+</u> and <u>PA</u>	50
6	Slow hydrolysis of <u>PA</u>	54
7	UV spectral scans of <u>PP+</u> \rightarrow <u>PA</u> at pH 7	55
8	UV spectrum of <u>PBH+</u> at ca. pH 2	56
9	pH-rate profile for <u>PP+</u> \rightleftharpoons <u>PA</u> , pH 0 - 14	59
10	Process (b) pH-rate profile for <u>PP+</u> and its derivatives	65
11	Chloroacetate buffer catalysis plots for process (c)	71
12	Process (d) pH-rate profile for <u>PP+</u> and its derivatives	78

Index to Schemes

No.	Content	page
1	Synthesis of the Pyrido-[1,2a]- Pyrimidinium Cations	2
2	An example of the synthesis of a pyrimidinium cation	4
3	Use of β -chlorovinyl ketones for synthesis of Pyrido-[1,2a]-pyrim- idinium cations	6
4	Addition of a primary amine to a carbonyl group	9
5	Type e mechanism for carbonyl hydration	14
6	Type n mechanism for carbonyl hydration	15
7	Proposed mechanism for process (a)	60

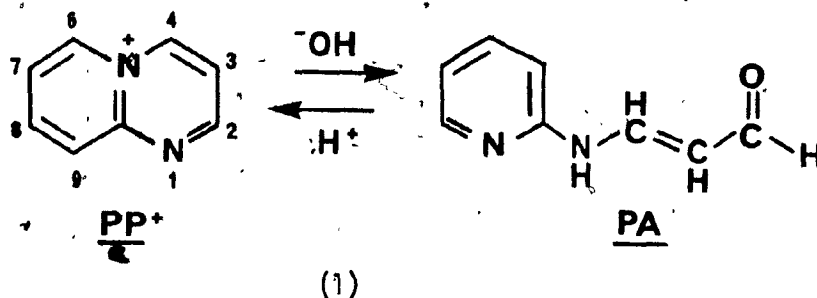
Index to Tables

No.	Content	page
1	Melting points of <u>PP+</u> and its derivatives	23
2	400 MHz NMR data for <u>PP+</u> and its derivatives	37
3	Coupling constants for Table 2	38
4	400 MHz NMR data for ring-opened compounds	39
5	Coupling constants for Table 4	40
6	¹³ C NMR data for <u>PP+</u>	41
7	60 MHz NMR data for <u>PP+</u> and its derivatives	42
8	400 MHz NMR data and K_{eq} values for the covalent hydrates of <u>PP+</u>	48
9	UV spectral data for <u>PP+</u> and its derivatives	51
10	UV spectral data for <u>PBH+</u>	57
11	Equilibrium Constants	63
12	k_{OH} values for <u>PP+</u> \rightleftharpoons <u>PA</u>	64
13	Rate constants calculated for buffer catalysis for process (c) - chloroacetate buffers	73
14-17	Rate constants for <u>PP+</u> processes (a) through (d)	88
18-24	Rate constants for the derivatives of <u>PP+</u>	92
25-29	Rate constants for buffer catalysis of <u>PP+</u> - process (c)	96

INTRODUCTION

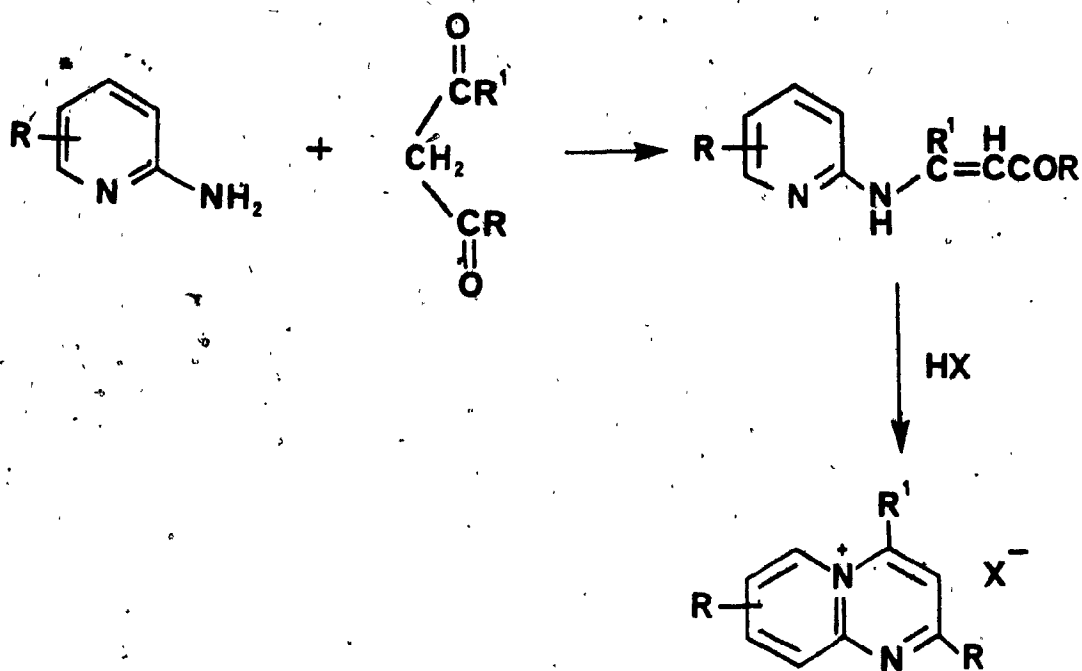
General Introduction

The object of this work was to study the kinetics and mechanism of the ring-opening reaction of the pyrido-[1,2a]-pyrimidinium cation (PP+) in aqueous base, and of the ring-closing of the 2-(2-pyridylamino)-acrolein (PA) under acidic conditions. Despite the fact that PP+ is of aromatic character, it easily ring opens in base.¹ However, PP+ is stable when heated in hydrochloric acid.²



Although the synthesis of pyrido-[1,2a]-pyrimidinium cations is well documented³, no attempt has been made to investigate the mechanism of eqn. 1. Clearly, elucidation of the pathway involved in the ring-opening of PP+ (and the ring-closing of PA) will be of use both synthetically and mechanistically. Moreover, as will be seen later, this study has relevance to the chemistry of tetrahedral intermediates.

A study of the NMR spectra (400 MHz) of PP+ and sev-



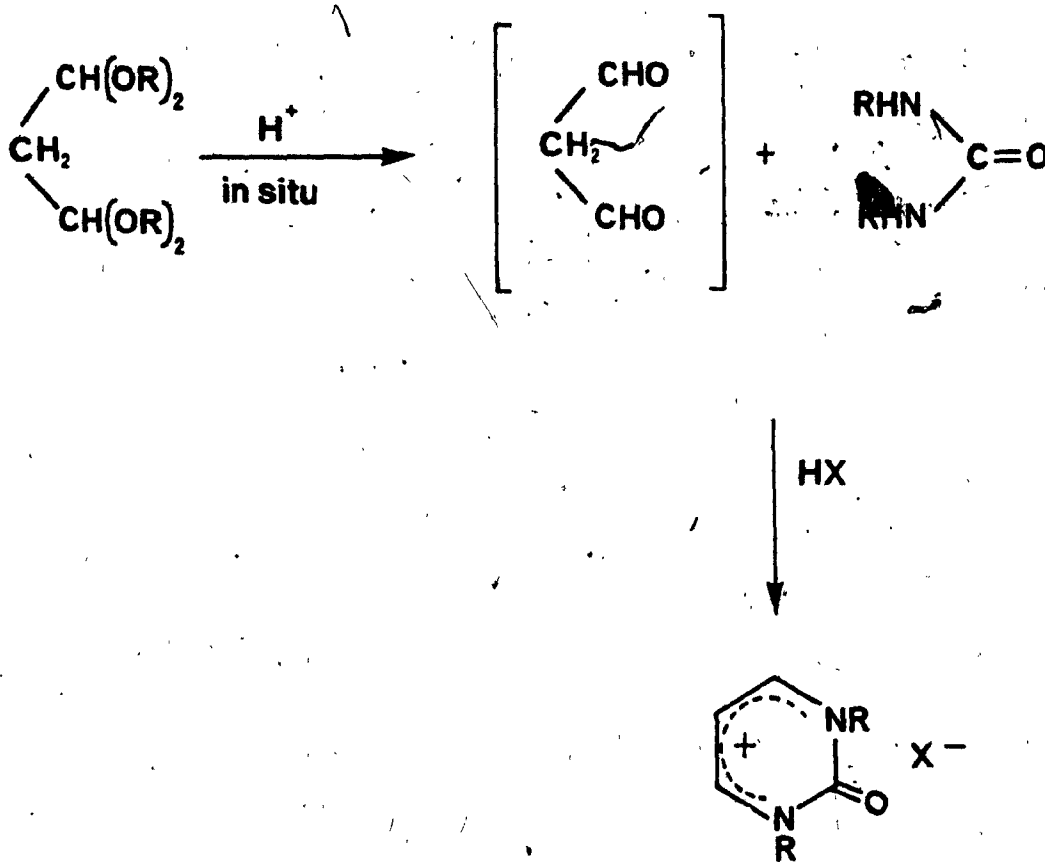
Scheme 1 Synthesis of the pyrido-[1,2a]-
Pyrimidinium cations

eral of its derivatives was also undertaken in order to clarify and add to the NMR data already present in the literature.¹

We corroborate some of the work of Tamura and Ono⁴ regarding the reactivity of the pyrido-[1,2a]-pyrimidinium cation, and use these data to aid in our investigation. Some substituted derivatives of PP+ were also studied to broaden the scope of this work.

Synthesis of the Pyrido-[1,2a]-Pyrimidinium Cations

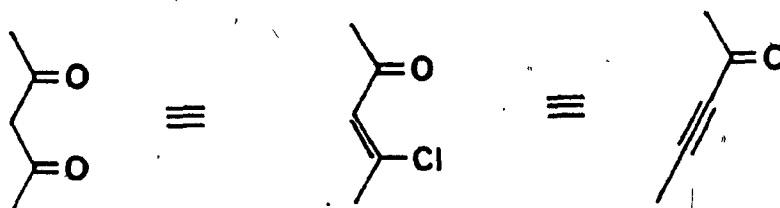
PP+ and many of its substituted derivatives¹ are easily synthesised from 2-aminopyridines and 1,3-dicarbonyl compounds in the presence of acid (Scheme 1).^{1,5} This type of reaction is similar to a general synthesis of pyrimidines and pyrimidinium cations, involving condensation of a urea or amidine and a 1,3-diketone under acidic or basic conditions.^{6,7,8} For example, reaction of malondialdehyde with N-alkylureas in acid, yields N-alkyl-2-pyrimidones, isolated as their salts (Scheme 2).⁶ With respect to the pyrido-[1,2a]-pyrimidinium cations, some investigators have been able to isolate the enamine intermediate in the absence of acid.^{1,5} Moreover, this type of compound (PA) can be obtained by



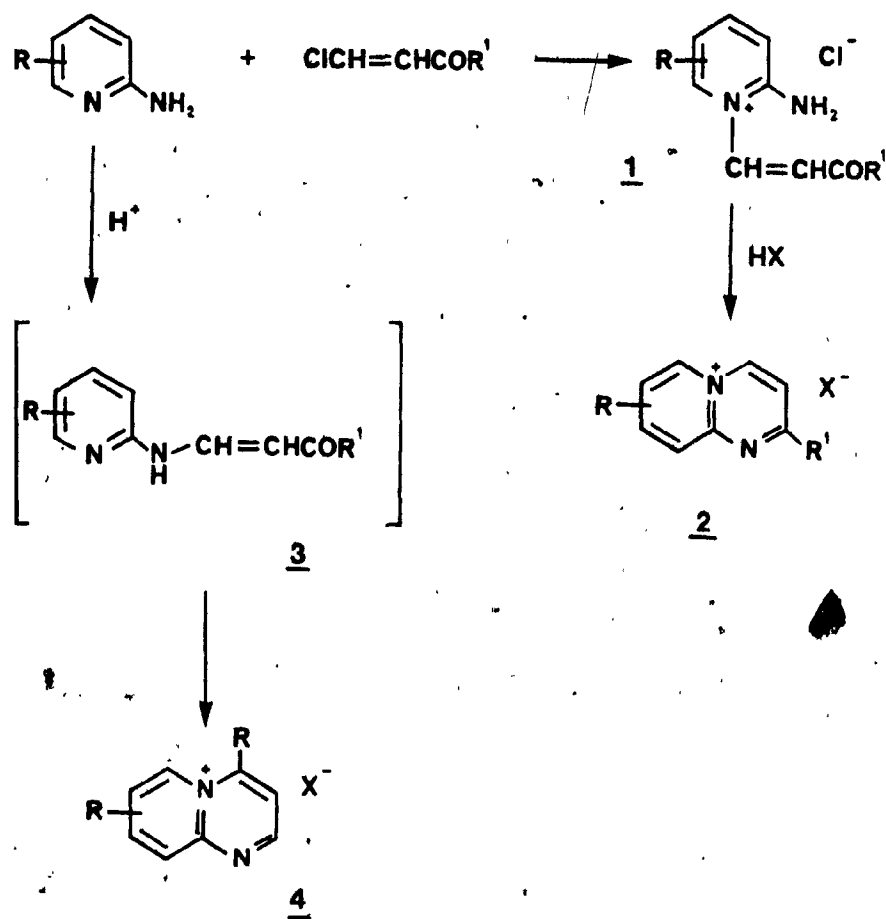
Scheme 2 An example of the synthesis of a Pyrimidinium cation ⁶

treating an aqueous solution of the iodide salt of the parent cation (\underline{PP}^+) with bicarbonate (Scheme 1).⁴

The use of substituted starting materials leads to the appropriately substituted pyrido-[1,2a]-pyrimidinium cations. For example, reaction of 2,3-diamino-5-bromopyridinium perchlorate with 2,4-pentanedione⁹ gives the appropriately substituted cation. Also, one can use other precursors in place of the 1,3-dicarbonyl component, if these are effectively at the same level of oxidation. Thus, β -chlorovinyl ketones (Scheme 3) and acetylenic ketones have both been used to prepare pyrido-[1,2a]-pyrimidinium cations.^{10,11}



In a literature search by Fischer¹², it was found that in a non-acidic environment (methanol/acetone), the pyridinium salts (1) are formed, which can be cyclised with acetic and 70% perchloric acids, yielding pyrido-[1,2a]-pyrimidinium cations substituted at position 2 (2). In acidic media however, intermediate enamine^{5,12} (3) formation leads to the 4-substituted compound (4).

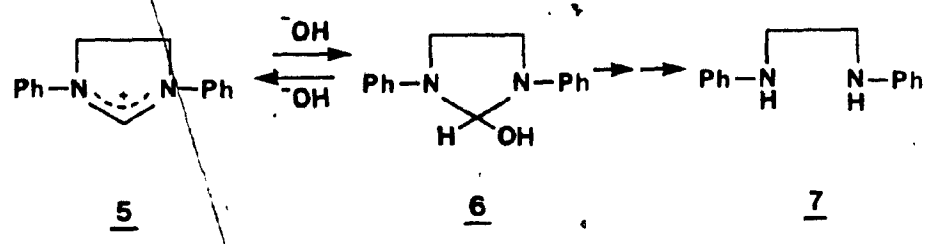


Scheme 3 Use of β -chlorovinyl ketones (aldehydes) for synthesis of pyrido-[1,2a]-pyrimidinium cations

Tetrahedral Intermediates and Pseudobase Formation¹³

The ring-opening (and reclosure) of PP+ probably involves its pseudobase, which is a tetrahedral addition intermediate. Such intermediates are now known to occur in many reactions of carbonyl compounds including aldehydes, ketones, carboxylic acids, esters, anhydrides, acyl halides, amides and others.^{14,15} It is also well known that transformations of carboxylic acid derivatives involving such intermediates play an important part in many biochemical processes.^{15,16} For this reason, reactions involving tetrahedral intermediates are of great interest.

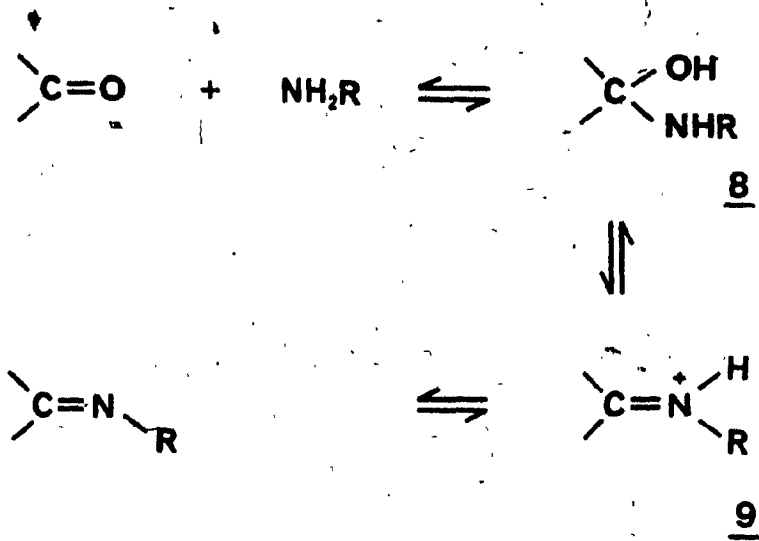
One of the earliest studies involving an observable tetrahedral intermediate was that by Robinson¹⁷ on the basic hydrolysis of 1,3-diphenyl-2-imidazolinium chloride (5) to form N-(2-anilonoethyl)-formanilide (7). However, Capon¹⁸ was unable to observe 6 by NMR using a mixed aqueous solvent system.



UV spectral evidence indicated the build-up of an intermediate which was suggested to be the tetrahedral intermediate (6) in the reaction above. More recently, tetrahedral intermediates have been directly observed in this laboratory by both NMR and UV methods, and these studies have involved ring-opening.¹⁹

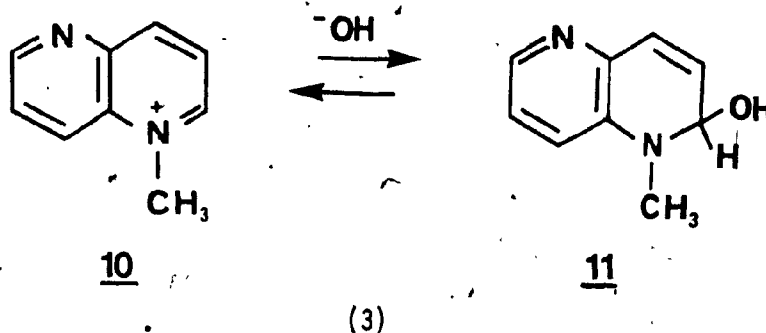
The formation of imines has also been established to involve a tetrahedral intermediate, in the form of a carbinolamine (8) (Scheme 4).²⁰ General examples of imines include oximes, hydrazones and semicarbazones. At one time these imines were used primarily to obtain solid derivatives of carbonyl compounds in the laboratory. More recently, the mechanisms involved in the formation of imines have been recognised to be a model for many important biochemical reactions.^{14,16} For example, imines (or Schiff bases) and their N-protonated forms, are proposed to be involved in the mechanism of addition of enzymes such as acetoacetate decarboxylase, aldolase, and transamination reactions with pyridoxalamine.¹⁶ Much work has gone into the study of the mechanisms involved in imine formation, and a wealth of material exists in the literature.^{16,20} Under acidic conditions, the iminium ion (9) is usually involved in the dehydration of the carbinolamine (8).

This type of reaction ($8 \rightleftharpoons 9$) is seen in the formation



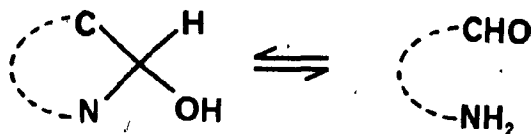
Scheme 4 Addition of a primary amine to a carbonyl group

of pseudobases from heterocyclic cations (eg 10 \rightleftharpoons 11).¹³



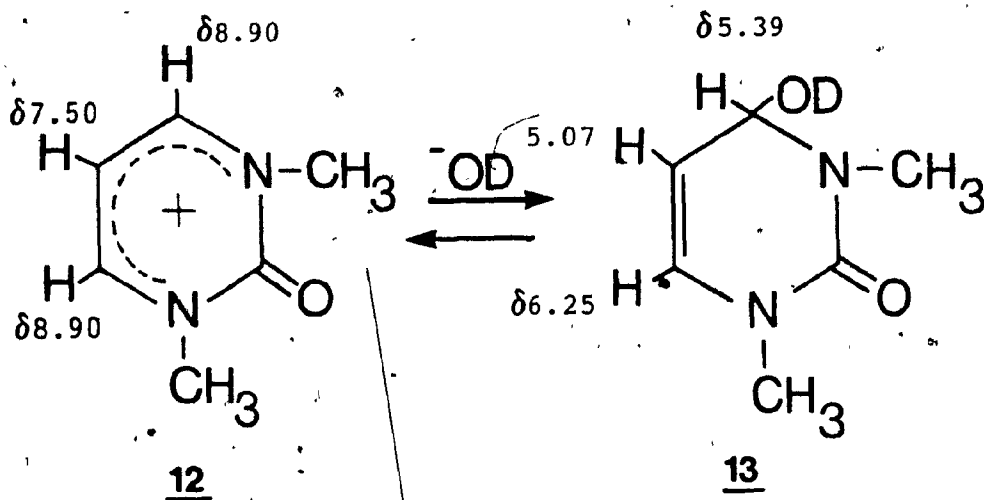
Pseudobases were first observed in the 1890s by Decker²¹ and Hantzsch²², for the acridinium and quinolinium cations. A typical example of pseudobase formation is found with the 1-methyl-naphthyridinium cation (10).²³

Pseudobase formation is a reversible, pH dependent process. Therefore, reacidification of a solution of the pseudobase will yield the parent cation. It is important, however, to be wary of ring-chain tautomerism when dealing with pseudobases. That is, under basic conditions, it is often possible for a pseudobase to undergo ring-opening to its aminocarbonyl tautomer (eqn. 4), which is an intramolecular analogue to the first step of Scheme 4.



In order to distinguish between the presence of the pseudobase and the ring-opened amino-carbonyl compound, Bunting¹³ has developed a simple test. By using basic methanol as solvent, the methoxide adduct of the heterocyclic cation is formed, which cannot undergo ring-opening in the same way. Therefore, if the UV spectra in aqueous base and in basic methanol show only minor differences due to solvent effects, then the pseudobase is the major form existing in basic aqueous solution. Major differences in the above spectra, however, indicate a significant amount of the ring-opened compound in basic aqueous solution.

NMR spectroscopy is also a useful tool in studying pseudobase formation, and many examples exist in the literature¹³. An upfield shift of ca. 4 ppm is observed when an unsaturated carbon bearing a hydrogen becomes saturated on forming the pseudobase. Protons nearby are also affected in a smaller, but similar manner. For example, in the case of the pseudobase (13) resulting from hydroxide ion addition to the 1,3-dimethyl-1,2-dihydro-2-oxypyrimidinium cation (12), the chemical shift of the proton at position 4 goes from 8.90 ppm to 5.39 ppm in the pseudobase (13). Smaller changes of chemical shift values are observed for protons at positions 5 and 6 as illustrated.⁶⁽ⁱ⁾



General Acid/Base Catalysis (Buffer Catalysis)^{14, 16, 20}

In the course of this investigation, a series of buffer catalysis experiments was carried out.

General acid/base catalysis is a widely used tool in the elucidation of organic reaction mechanisms. It has been employed in the study of alkene hydration, hydrolysis of esters and amides, and the reactions of nucleophiles with carbonyl compounds²⁰ (cf. Scheme 4), to mention a few examples.

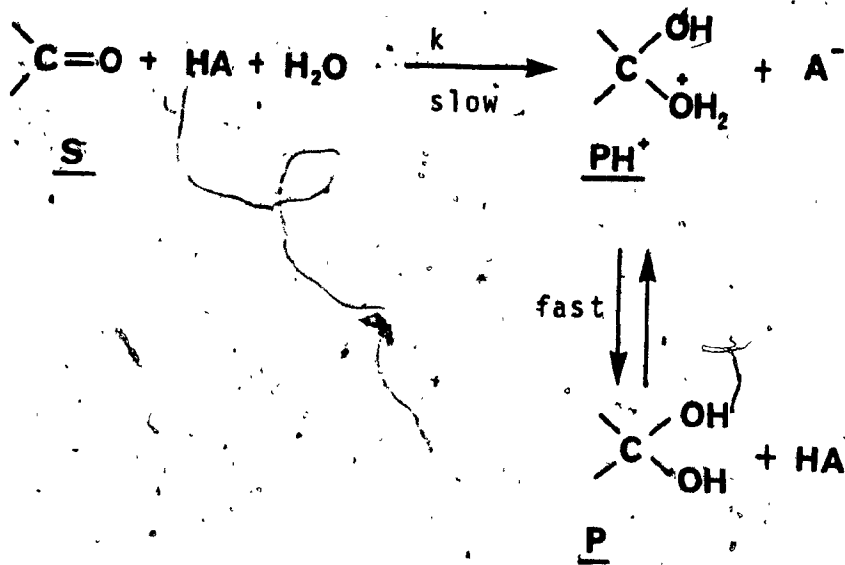
General species catalysis is involved when a reaction rate increases with increasing buffer concentration at constant pH. It may be due to the buffer acid or the buffer base (or both). Specific catalysis in aqueous solution, on the other hand, involves catalysis by only

H_3O^+ or OH^- ions.

In the case of the hydrolysis of ethyl dichloroacetate²⁴, general base catalysis was found. A plot of k^{obs} versus [base] gave straight lines for both acetate ion and pyridine. The slope of these lines gives k_2 , the second order rate constant for general base catalysis. The intercept at zero buffer concentration is the rate constant due to OH^- catalysis and any catalysis by the solvent. A plot of such intercepts versus $[OH^-]$ yields the rate constants for the solvent and OH^- catalysed reactions.

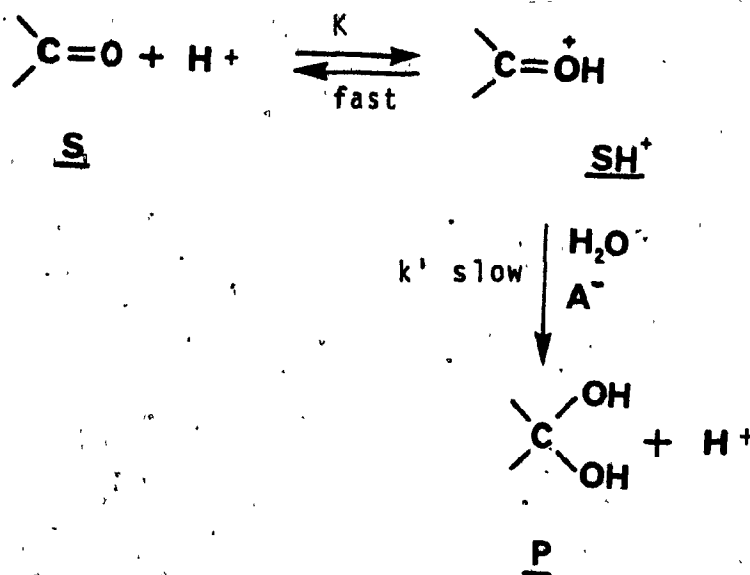
It is important to realise that while general catalysis often indicates a slow (rate determining) proton transfer, specific catalysis does not necessarily involve any proton transfer in the rate determining step. It may be occurring in a pre-equilibrium step.

There exist mechanistic ambiguities in general catalysis. For example, general acid catalysis is kinetically indistinguishable from combined specific acid and general base catalysis. Jencks^{20,25} has outlined two possible mechanisms for carbonyl hydration which illustrate this point (Schemes 5 and 6). The type e mechanism involves rate-limiting general acid catalysed attack of water (acting as a nucleophile), followed by proton loss to the gem-diol product. Conversely, the type n mechanism is



$$\begin{aligned}
 \text{rate} &= k[\text{S}][\text{HA}][\text{H}_2\text{O}] \\
 &= k^{\text{obs}}[\text{S}][\text{HA}]
 \end{aligned}$$

Scheme 5. Type e mechanism for carbonyl hydration



$$\begin{aligned}
 \text{rate} &= k' [\text{SH}^+] [\text{A}^-] [\text{H}_2\text{O}], \\
 &= \frac{k' K [\text{S}] [\text{H}_2\text{O}] [\text{HA}]}{K_{\text{HA}}} \\
 &= k^{\text{obs}} [\text{S}] [\text{HA}]
 \end{aligned}$$

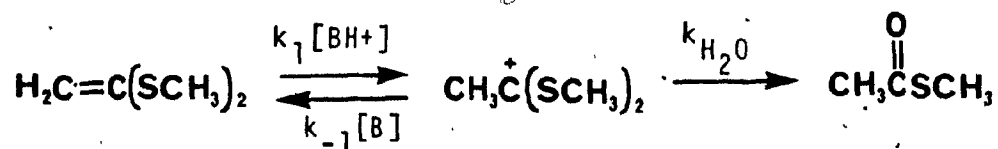
$$K = \frac{[\text{SH}^+]}{[\text{S}] [\text{H}^+]}$$

$$K_{\text{HA}} = \frac{[\text{H}^+] [\text{A}^-]}{[\text{HA}]}$$

Scheme 6. Type n mechanism for carbonyl hydration

comprised of specific acid protonation of the carbonyl oxygen, followed by rate limiting general base catalysed water attack to form the product. The rate expression for the above two mechanisms are mathematically equivalent and so these mechanisms are kinetically indistinguishable. Fortunately, there exist means²⁰ to determine which of the above two mechanisms is occurring, such as measurement of solvent isotope effects, Brønsted exponents, etc.

Curved plots of k^{obs} versus [buffer] showing saturation at higher buffer concentrations were obtained in the present study. Similar plots have been observed previously²⁶ and they have been associated with a change of rate-determining step with increasing concentration of buffer. An example of this type of behavior was recently found by Okuyama et al²⁶ studying the acid-catalysed hydrolysis of 1,1-bis (methylthio) ethane.



(6)

Kinetic analysis suggests a change of rate-determining step from protonation of the double bond at low [buffer], to hydration of the intermediate carbonium ion at high [buffer], as follows:

Assuming the cation is only present in steady-state

amounts²⁰,

$$k^{\text{obs}} = k_1[\text{BH}^+] k_{\text{H}_2\text{O}} / (k_{-1}[\text{B}] + k_{\text{H}_2\text{O}}).$$

This equation will give rise to curved buffer plots if at low [B] the term $k_{-1}[\text{B}] \ll k_{\text{H}_2\text{O}}$, but at high [B] the inequality is reversed ($k_{-1}[\text{B}] \gg k_{\text{H}_2\text{O}}$).

The former corresponds to rate-limiting formation of the cation, whereas the latter refers to its rate-limiting hydration.

The Stopped-Flow Method

For the most part, the reactions monitored in this work occur quite rapidly, and so required the use of the stopped-flow technique.

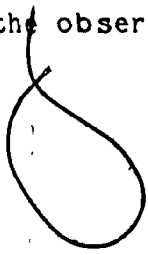
This method can be used to monitor chemical reactions with half lives of a few milliseconds up to several minutes. It involves the rapid mixing of two reactant solutions immediately prior to entering the observation chamber, followed by rapid stoppage of the flow, whereupon observation and data acquisition begin. A very short mixing time and short "dead" time, as well as sudden flow stoppage are required in order to follow very fast processes. The flow must be stopped abruptly, as a gradual decrease in flow rate may lead to incomplete

mixing. That is, if the reacting solutions are not thoroughly mixed before the observation point is reached, a lower than actual rate will be obtained.²⁷

The stopped-flow apparatus designed by Gibson²⁸, is the prototype of most of the equipment in use today. It initially employed a spectrophotometric observation system, although E.M.F. measurements^{29,30} have since been used as well.

A somewhat similar technique for following fast reactions is the continuous flow method, first applied to solution kinetics sixty years ago.³¹ As with stopped flow, two reacting solutions are forced together, but the resultant mixture is observed at various positions along the reaction tube. The distance the reaction is measured from the point of mixing determines the extent of reaction. Continuous flow requires substantial volumes of solution: anywhere from 20-500mL per run, depending upon reaction time and observation tube diameter.²⁷ This technique has recently found usage in monitoring reactions by NMR spectroscopy.³²

In contrast, the stopped flow method requires very little solution -- an important consideration when reactants are expensive, or difficult to prepare. The stopped flow technique is also free from the effects of the character and rate of flow through the observation tube, and is not



affected by mechanical disturbances.³³

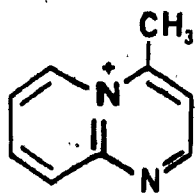
In summary, when equipped with a suitable observation and data acquisition system (vide infra), the stopped flow apparatus allows the study of reactions with half lives as short as several milliseconds. This technique was used extensively for the determination of kinetic data in this thesis.

EXPERIMENTAL

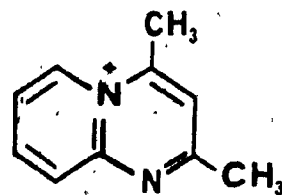
Melting points were determined on a Gallenkamp melting point apparatus and are uncorrected. ^1H NMR spectra were recorded on a Bruker WH-400 (Université de Montréal) or on a Bruker WP-80SY (Concordia). ^{13}C NMRs were run on the Bruker WP-80SY. Static UV spectral scans, for the determination of peak positions and extinction coefficients were recorded on a Perkin-Elmer 552 UV-Visible spectrophotometer, coupled to a Watanabe SR 6254 strip chart recorder. The apparent pK_a between PP^+ and PA was determined on a Cary 2290 UV-Visible Spectrophotometer, as were some of the very slow reactions corresponding to ring opening and closing of PP^+ . These kinetic experiments duplicated the conditions used in the stopped flow experiments, in that the substrate solution and buffer were mixed 1:1 and the temperature was maintained at 25°C . Non-routine chemicals were obtained from Aldrich and Eastman.

Materials

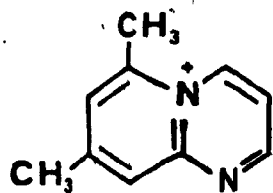
The Pyrido-[1,2a]-pyrimidinium cation and several of its derivatives (Figure 1) were prepared in good yield following Sawyer and Wibberley,¹ as outlined in Scheme I. Melting points are given in Table 1 below. PP^+ perchlorate



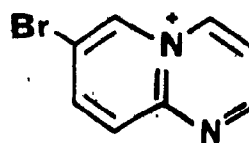
4-Me-PP+



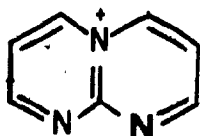
2,4-diMe-PP+



6,8-diMe-PP+



7-Br-PP+



PP+

Figure 1. Several derivatives of PP+

was synthesised by reacting 2-aminopyridine with malondialdehyde bis-(dimethyl acetal) in methanol containing a slight excess of perchloric acid, the reaction was stirred overnight at room temperature.

The 4-methyl (MPP+) and 2,4-dimethyl (DMPP+) derivatives of PP+ were made as above, substituting acetyl acetaldehyde (dimethyl acetal) and 2,4-pentanedione respectively, for malondialdehyde bis-(dimethyl acetal). The iodide salt of PP+ was also synthesised using hydriodic acid in place of perchloric acid, and refluxing the reaction for three hours. Pyrimido-[1,2a]-pyrimidinium perchlorate (P+) (Figure 1) was synthesised as above, using 2-aminopyrimidine. We were unable to synthesise the 7-nitro derivative of PP+, even after refluxing for eight hours.

Two previously unreported derivatives of PP+ were prepared in the above manner. 7-Br-PP+, both the iodide and the perchlorate salts, were made using 2-amino-5-bromopyridine and refluxing for three hours. 6,8-dimethyl-PP+ was made using 2-amino-4,6-dimethylpyridine and stirring overnight at room temperature. NMR spectra taken at 400 MHz, as well as UV spectra, support the assigned structures (vide infra).

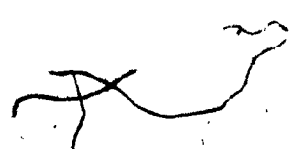


Table 1. Melting Points of PP+ and Derivatives

Compound ^a	M.P. (°C)	M.P. (literature) ¹
<u>PP+</u>	210-214	216
4-Me- <u>PP+</u>	215-220 (decomp)	232-233
2,4-diMe- <u>PP+</u>	224-225 (decomp)	228-230
6,8-diMe- <u>PP+</u> ^b	213-215	-----
7-Br- <u>PP+</u> ^b	201-203	-----
<u>PP+</u> I-	decomp > 200	-----
7-Br- <u>PP+</u> I-	decomp > 200	-----

^aRefers to the perchlorate salts, unless indicated otherwise.

^bElemental analysis (Galbraith Laboratories) gave the following: 6,8-diMe-PP+ calc: C, 46.42; N, 10.86; H, 4.29. found: C, 46.28; N, 10.64; H, 4.22. 7-Br-PP+I- calc: C, 28.51; N, 8.38; H, 1.79; Br, 23.71; I, 37.65. found: C, 28.31; N, 8.13; H, 1.90; Br, 23.67; I, 38.12

PA was synthesised from PP+ by the method of Tamura and Ono.⁴ The iodide salt of PP+ was dissolved in water and bicarbonate was added to this solution until a precipitate of PA formed. PA was recrystallised from water before use.

Kinetic Solutions

All kinetic solutions were prepared with glass distilled water and the total ionic strength was maintained at 1.0 M, using NaCl. Solutions above pH 11 or below pH 2 were made by diluting stock 1N NaOH or 1N HCl (A&C American chemicals) respectively. After taking into account 1:1 dilution in the stopped flow, the pH was calculated.

An adjustment of the calculated pHs was made to reflect the 1M ionic strength of the media used. At high pH (pH > 11) the correction is of the form³⁴

$$\text{pH} = \text{pH}_{\text{calc}} - 0.15. \quad (7)$$

At low pH, a modified form of the Debye-Huckel equation³⁵ due to Davies, was used to correct the activity coefficient f_1 , such that,

$$-\log f_1 = Az^2 I^{.5} / (1 + I^{.5}) - 0.1z^2 I \quad (8)$$

where A is a constant 0.512 at 25°C, I is the ionic strength, and z is the ionic charge. The value of f_1 so calculated is substituted into the equation

$$a_i = c_i f_i \quad (9)$$

where a_i is the activity of the ion, and c_i is its concentration. A computer programme written in BASIC was used to correct calculated pHs according to the above treatment, to account for the 1.0 M ionic strength of the media.

In the range of pH 2-11, buffers (0.02M before mixing) were prepared according to Perrin.³⁶ These included chloroacetate (pH 2.20-3.40), acetate (pH 4.10-5.30), succinate (pH 3.60-6.20), phosphate (pH 6.40-7.70), borate (pH 8.50-9.70), and carbonate (pH 9.60-10.60). The pHs of these solutions, after mixing 1:1 with substrate solutions were measured with a Corning Digital 110 Expanded Scale pH meter, calibrated with the appropriate standard buffers.

Buffer catalysis experiments employed parent buffers ~~of~~ up to 0.4M buffer strength before mixing. Due to the relatively high concentration of these buffers, they were prepared using the Henderson-Hasselbach equation,³⁷

$$\text{pH} = \text{pK}'_a + \log[A^-]/[HA], \quad (10)$$

where pK'_a is the pK_a at 1M ionic strength. The parent buffers were subsequently diluted to give buffers of lower concentration. For buffer catalysis experiments carried out at low pH, cyanoacetate ($\text{pK}'_a = 2.23$),³⁸ dichloroacetate ($\text{pK}'_a = 1.14$)³⁹ and formate ($\text{pK}'_a = 3.62$)⁴⁰ buffers were used.

Determination of the Apparent pK_a between PP^+ and PA .

Several methods exist for the determination of ionisation constants (pK_a s) including potentiometry, conductimetry, and spectrophotometry.⁴¹ A system such as $PP^+ \rightleftharpoons PA$ is well suited to the spectrophotometric method, as spectral differences between the two species are large. Also, equilibration at certain pHs are quite slow, making potentiometric determination of the ionisation constant tedious.

PP^+ solutions ($5 \times 10^{-5} M$, $I = 1.0 M$ (NaCl)) were prepared in a series of non-absorbing buffers of varying pH and were allowed to reach equilibrium for 44 hours at room temperature. The absorbance of these solutions was then measured at two analytical wavelengths: 225nm and 325nm. Calculation of the apparent pK_a , performed in the usual way,⁴¹ gave 5.90 ± 0.1 .

Kinetic Apparatus

Except for the very slow reactions, all kinetic runs were carried out using an Aminco-Morrow Stopped-Flow accessory⁴² fitted to an Aminco DW-2 UV-Visible spectrophotometer, operated in a double beam mode. In contrast

to the conventional sample versus reference cuvette system, the double beam mode utilises a monitoring and a reference wavelength, which are alternately passed through the sample by means of a chopper. The emergent light beams are then compared by the detection system. The reference wavelength is chosen such that little or no absorbance change is seen there, while the other monochromator is set where a large change in absorbance occurs. Normally the chopper operates at 250 Hz, but for reactions with a total reaction time of less than 5 seconds, the chopper speed is increased to 1,000 Hz.

The advantages of the dual wavelength system are as follows:

- a) It eliminates the need for a reference solution.
- b) Since both monitoring beams are derived from the same light source, fluctuations in light intensity, amplifier gain and detector response are minimised.^{43,44}
- c) Instrumental artefacts due to light scattering in turbid solutions are minimised, as both beams pass through the same sample.⁴⁵ This is especially beneficial to those working with biological or biochemical preparations.

The stopped flow apparatus was used with one drive syringe filled with 2mL of substrate solution and the other with 2mL of the appropriate acid, base, or buffer.

These solutions were driven together under a nitrogen pressure of 58-60 psi into a 10mm long observation cell. The volume monitored spectrophotometrically was 0.4mL.⁴² Under these conditions, the "dead time" of the system is approximately 4 milliseconds. That is, about 4 msec. are required before the reactants are thoroughly mixed and reach the point of observation. The stopping of the solution flow is controlled by a micrometer with a trigger switch mounted in its tip. When the piston of the exit syringe advances, as the two solutions are mixed, the micrometer switch is closed and data acquisition begins.

Kinetic Procedure and Data Acquisition

All kinetic runs were carried out at 25.0°C to within 0.1°C. This temperature was maintained with a Lauda RC-20B constant temperature circulating water bath. All reactants were allowed to temperature equilibrate in the stopped-flow apparatus prior to carrying out kinetics.

The sample and reference monochromator on the DW-2 were set according to the process being followed. In most cases, the concentration of the substrate was $5 \times 10^{-5} \text{M}$ after mixing 1:1 with acid, base, or buffer. For reactions

monitoring ring closing, the cation was allowed to ring-open in 0.001N NaOH before proceeding. Ring-closing reactions were also carried out using an authentic sample of PA, employing a concentration of 1×10^{-4} M. In all cases, pseudo-first order kinetics were obtained owing to the large excess of acid, base, or buffer over the substrate.

For reactions with a half-life of less than 20 seconds a data acquisition system was used to monitor the kinetics (Figure 2). For each reaction, absorbance changes from the DW-2 were recorded on a Biomation 605 digital waveform recorder and the stored trace (2048 points) was displayed on a Tektronix 2215 60 MHz oscilloscope. Acceptable traces were transferred serially at 9600 baud via a Datas 305 interface to an Apple II microcomputer. The Apple extracted every twentieth point (100 points total) from the 2048 points transferred and obtained an average infinity value from the last 10 points. First order rate constants were then calculated using approximately 16-40 points comprising ca. 85-95% reaction (usually 90%) with the TR1ST programme. For the purposes of record keeping, traces from the Biomation were plotted on an X-Y recorder.

Reactions with a half-life greater than 20 seconds were recorded directly onto an X-Y recorder. Rate constants were determined by hand digitising ca. 20

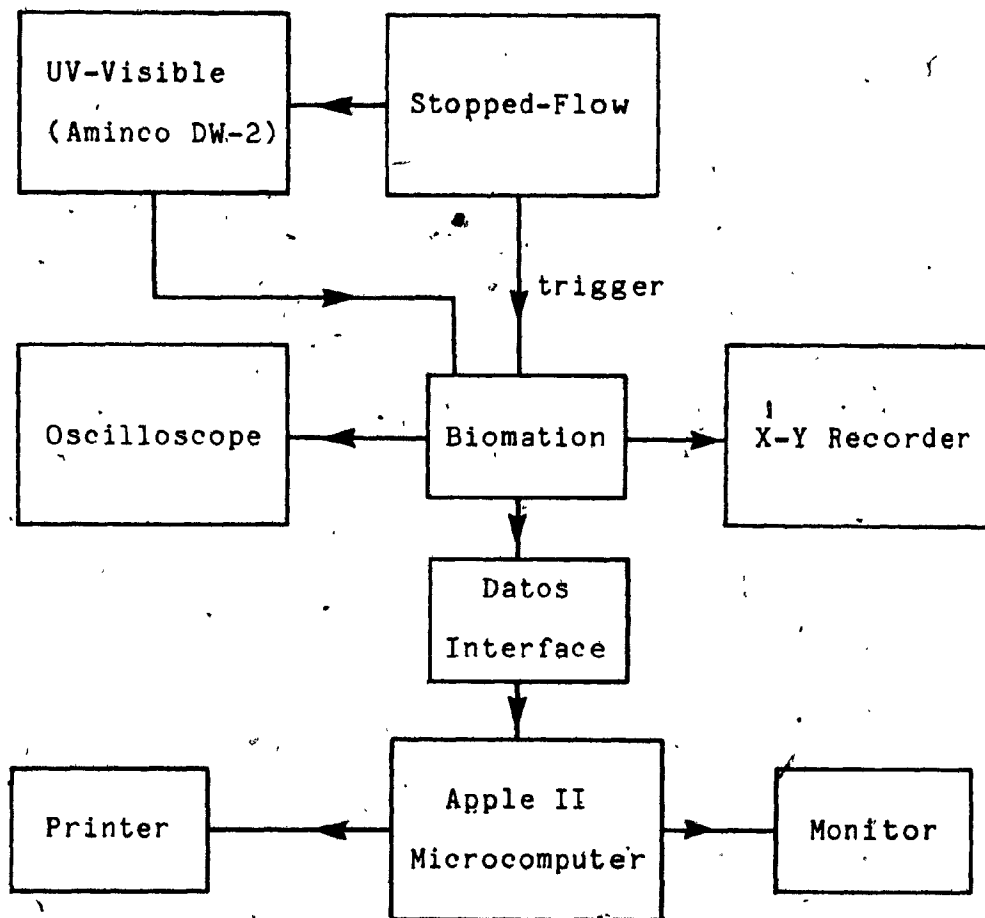


Figure 2. Stopped-Flow Data Acquisition System

points corresponding to 85-95% (usually 90%) reaction and analysing these data using the FIRST programme on the Apple, or the NEW1ST programme on the Cyber 170 mainframe computer. For the very slow reactions studied, the conventional method of a sample and reference cuvette was used with the DW-2 to determine kinetic data. As with stopped flow experiments, substrate and buffer were mixed in a ratio of 1:1. Some of the slow reactions were also followed using a Cary 2290 UV Spectrophotometer in the conventional sample versus reference mode.

Computer Programmes

In the programmes TR1ST, NEW1ST, and FIRST, the first order rate constants were calculated using Guggenheim, Swinbourne, "Normal", and "Normal" with Swinbourne calculated infinity methods (vide infra).

Rate and equilibrium constants were calculated by fitting derived rate equations to the experimental points obtained using the PROFIT programme, or variations thereof. This is an iterative programme designed to give the best curve to a given set of data using standard non-linear least squares techniques.⁴⁶

All computer programmes used throughout the course

of this work were written in BASIC and machine language by Professor O.S. Tee, with the exception of the NEWIST programme, which was written in FORTRAN. Aside from a few determinations of rate constants done on the Cyber 170 mainframe computer, an Apple II microcomputer was used for all calculations.

Treatment of Kinetic Data

The computer programmes used for calculating first order rate constants used three different methods. Each of these will be briefly outlined in this section.

1. "Normal" Treatment of Kinetic Data⁴⁷

For a first order reaction which follows the Beer-Lambert Law, the change of absorbance with time follows the equation

$$(A - A_{\infty}) = (A_0 - A_{\infty})e^{-kt} \quad (11)$$

Taking natural logarithms gives

$$\ln(A - A_{\infty}) = \ln(A_0 - A_{\infty}) - kt. \quad (12)$$

where A_0 is the absorbance at zero time ($t=0$),

A_{∞} is the final absorbance,

A is the absorbance at time t , and

k is the first order rate constant.

From eqn. 12 it can be seen that a plot of $\ln(A - A_\infty)$ versus time should give a straight line of slope $-k$.

In order to analyse kinetic data in such a way, an accurate value of A_∞ is required. Small variations in A_∞ can greatly affect the rate constant while leaving the least squares correlation coefficient relatively unchanged. Collins found that an error of one part in A_∞ can be magnified up to fourteen times in the rate constant.⁴⁸

2. Swinbourne Treatment of Kinetic Data⁴⁹

Both the Swinbourne and Guggenheim treatments of data find their utility in that no value for A_∞ is required. Therefore, they allow the experimenter to study reactions where the final absorbance is not measurable, for whatever reason. However, they should only be used where it is virtually certain that a first order reaction is involved. Otherwise spurious results will be obtained.

If, for a first order reaction, A_1, A_2, \dots, A_n are the absorbance readings corresponding to times t_1, t_2, \dots, t_n , and A_1', A_2', \dots, A_n' are another series of absorbances for $t_1+T, t_2+T, \dots, t_n+T$, where T is constant, then we have

$$(A' - A_\infty) = (A_0 - A_\infty)e^{-k(t+T)}. \quad (13)$$

Dividing eqn. 11 by eqn. 13 gives

$$(A - A_\infty)/(A' - A_\infty) = e^{kT} \quad (14)$$

and therefore

$$A = A_{\infty}(1 - e^{-kT}) + A'e^{kT} \quad (15)$$

From eqn. 15 a plot of A versus A' should give a straight line of slope e^{kT} and intercept $A_{\infty}(1 - e^{-kT})$. Obviously k can be obtained from the slope and from the slope and intercept:

$$A_{\infty} = (\text{intercept}) / (1 - \text{slope}). \quad (16)$$

For optimal results T should be between 0.5 and 1 half-life and the data should cover more than one half-life, preferably more than 2.⁴⁹

3. Guggenheim Treatment of Kinetic Data^{47,49}

This method, as the one above, allows the calculation of a first order rate constant without using a measured A_{∞} .

Subtracting eqn. 11 from eqn. 13 yields

$$(A' - A) = (A_0 - A_{\infty})e^{-kt}(e^{-kT} - 1) \quad (17)$$

Taking logarithms gives

$$\begin{aligned} \ln(A' - A) &= \ln((A_0 - A_{\infty})(e^{-kT} - 1)) - kt \\ &= \text{constant} - kt \end{aligned} \quad (18)$$

Therefore, a plot of $\ln(A' - A)$ versus t should give a straight line of slope $-k$. For best results data should cover greater than 2 half-lives, and T should be 0.5 to 1 half-life.⁴⁸

Kinetic constants determined in this work utilised the "Normal" method whenever possible. If the observed

A_{∞} value was found to drift due to a subsequent reaction, or for instrumental reasons, a Swinbourne calculated infinity value was used in the "Normal" treatment of data.

Replicate rate constants were usually found to be within 5 % of each other, and analysis of $\ln(A - A_{\infty})$ versus t had a least squares correlation coefficient of at least 0.999 in most cases. Each rate constant determined is the average of at least 3 (usually 4) trials, except for the very slow reactions, where duplicate measurements were taken.

RESULTS AND DISCUSSION

Introduction

The pyrido-[1,2a]-pyrimidinium cation and several of its derivatives (4-Me, 2,4-diMe, 7-Br, shown on page 21), were studied over the pH range 0-14 with respect to their ring-opening in basic solution and their ring-closing in acidic solution.

NMR and UV spectroscopy were used throughout the course of this investigation, both statically and dynamically. This section presents the results of these experiments and proposes mechanisms to account for the data obtained, where possible.

1. NMR Studies

Below are tables (Tables 2-6) containing NMR data for the pyrido-[1,2a]-pyrimidinium cations investigated, as well as for several of the ring opened compounds. Table 6 contains some ^{13}C NMR data. Sawyer and Wibberley¹ have presented extensive spectral information in this area, but as their spectra were recorded at 60 MHz (in trifluoroacetic acid), not all proton resonances were well separated and most coupling constants were not resolvable (see Table 7). We therefore undertook an NMR study of these compounds to clarify and add to the data already present in the literature.¹ In addition, the 400 MHz instrument made

Table 2. 400 MHz NMR Data for PP+ and its Derivatives^{a,b}

Compound	2H	3H	4H	6H	7H	8H	9H
<u>PP+</u>	9.52 d,d	8.21 d,d	9.66 d,d	9.32 br,d	8.22 d,d	8.66 d,t	8.56 d
<u>7-BrPP+</u>	9.49 d,d	8.24 d,d	9.54 d,d	9.78 d	----- -----	8.85 d,d	8.51 d
<u>2,4diMePP+</u>	Me ^c 2.82	8.08 s	Me 2.99	9.24 d	8.11 d,t	8.60 d,t	8.43 d,d
<u>6,8diMePP+</u>	9.45 d,d	8.08 d,d	9.53 br,d	Me 2.96	8.07 s	Me 2.71	8.34 s
<u>4-MePP+</u>	9.42 d	8.16 d	Me 3.06	9.34 d	8.22 d,t	8.68 m	8.59 d,d
(<u>P+</u>)	9.69 d,d	8.32 d,d	9.77 d,d	*	*	*	-----
<u>7-BrPP+</u> ^e	9.44 ^f br,m	8.15 m	2H	9.48 br,m	-----	8.78 m	8.47 m
<u>PP+I-</u> ^e	9.52 ^f br,m	8.15 d,d	2H	9.19 d	8.21 m	8.70 m	8.56 d

^acoupling constants are given in Table 3.

^bsamples in DMSO-d₆ except where indicated otherwise

^cMe = methyl group (singlet)

^esample run in D₂O -- calibrated with DSS

^fincludes resonance due to 4H

*Symmetrical compound

s = singlet, d = doublet, t = triplet, m = multiplet
br = broad, d,d = doublet of doublets, d,t = doublet triplets

Table 3. Coupling Constants (Hz) for Table 2^a

Compound	J _{2,3}	J _{2,4}	J _{3,4}	J _{6,7}	J _{6,8}	J _{7,8}	J _{8,9}
<u>PP+</u>	4.2	1.7	6.9	6.6	1.4	7.4	8.6
<u>7-BrPP+</u>	4.3	1.7	6.9	---	2.1	---	9.3
<u>2,4diMePP+</u>	---	---	---	7.0	n.o.	7.2	8.7
<u>6,8diMePP+</u>	4.1	1.6	7.2	---	---	---	---
<u>4-MePP+</u> ^b	4.5	---	---	6.9	n.o.	7.0	8.7
<u>(P+)</u>	6.7	2.0	4.3	---	---	---	---
<u>7-BrPP+</u> ^c	n.r.	n.r.	n.r.	n.r.	n.r.	n.r.	n.r.
<u>PP+I-</u> ^c	4.4	n.r.	6.9	6.7	n.r.	7.5	8.8

^a samples run in DMSO-d₆, unless otherwise indicated

^b J_{7,9} = 1.5 Hz

^c samples run in D₂O

n.o. = not observed, n.r. = not resolvable

Table 4. 400 MHz NMR Data for Ring-Opened Compounds^{a, b}

Compound	N-H	ald ^c	H _α	H _β	3H	4H	5H	6H
(P ⁺) ^e	10.87 br, d	9.35 d	5.73 d, d	8.3 ^f	-----	8.59 d	7.09 t	8.59 d
PA ^b	10.53 d	9.28 d	5.60 br, t	8.46 br, t	6.92 d	7.71 m	6.99 d, d	8.25 d, d
PA ^g	n.o. ^h	9.03 d	5.74 d, d					
(Br) ^{b, i}	10.62 d	9.29 d	5.61 d, d	n.o.	6.90 d	7.91 d, d	-----	8.35 d

^aCoupling constants are given in Table 5.

^bsamples run in DMSO-d₆, except where indicated -- spectrum calibrated on solvent peaks

^caldehydic (formyl) hydrogen

^eobserved in situ with parent cation

^fapproximate value -- obscured by resonances due to parent cation

^grun in D₂O at 80 MHz -- not all resonances well separated

^hn.o. = not observed (exchanged with D₂O solvent)

ⁱBr = ring-opened form of 7-BrPP+

d = doublet, t = triplet, m = multiplet,
br = broad, d, d = doublet of doublets

Table 5. Coupling Constants (Hz) for Table 4

Compound	$J_{\text{NH},\text{H}}$	$J_{\text{ald},\text{H}}$	$J_{\text{H}_\alpha,\text{H}_\beta}$	$J_{3,4}$	$J_{4,5}$	$J_{4,6}$	$J_{5,6}$
<u>(P⁺)</u> ^a	11.6	8.5	13.6	----	4.8	n.o.	4.8
<u>PA</u> ^a	ca. 12	8.5	ca. 12.5	8.2	7.2	1.8	5.0
<u>PA</u> ^{b,c}	n.o.	9:1	13.6				
<u>(Br)</u> ^{a,d}	11.6	8.5	12.9	8.7	----	2.5	----

^a recorded in DMSO-d₆

^b recorded at 80 MHz; all others are at 400 MHz

^c recorded in D₂O

^d Br = ring-opened form of 7-BrPP⁺

Table 6. ^{13}C NMR data^{a,b} (@ 20.15 MHz)

Compound	Position							
	C2	C3	C4	C6	C7	C8	C9	C9a
(P+) ^c	145.9	119.8	165.7	*	*	*	----	150.0
PP+ClO4- ^c	142.9	124.0	160.8	144.1	119.0	137.2	127.3	148.3
PP+I- ^e	142.5	124.8	161.0	143.6	119.4	136.7	127.5	148.3

* symmetrical compound

^a recorded at a ^1H spectrometer frequency of 80 MHz

^b spectral assignments by analogy to G.C. Levy, R.L. Lichter and G.L. Nelson, "Carbon-13 Nuclear Magnetic Resonance Spectroscopy", 2nd edition, J. Wiley and Sons, New York, 1980.

^c in DMSO-d₆ -- Calibrated on solvent signal

^e in D₂O -- Calibrated on acetone signal in D₂O

Table 7. 60 MHz NMR Data for PP+ and its Derivatives³

Compound	2H	4H	6H	8H	9H	3H	7H
<u>PP+</u> ^a	9.63 - 9.41		9.17	8.79	8.56	(8.36 - 8.03)	
<u>4-MePP+</u> ^b	9.45	Me	9.25	(8.82 - 8.62)		8.13	8.31
<u>2,4-diMePP+</u> ^c	Me	Me	9.13	(8.75 - 8.45)		7.98	8.17

^a $J_{6,7} = \text{ca. } 7 \text{ Hz.}$

^b $J_{2,3} = 5.0 \text{ Hz, } J_{6,7} = 7.4 \text{ Hz, Me at } 3.22 \text{ ppm.}$

^c $J_{6,7} = 7.0 \text{ Hz, Me at } 2.98, 3.13 \text{ ppm.}$

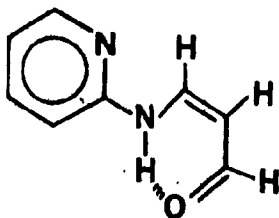
possible the observation of species present in very small amounts. Spectral assignments were made on the basis of chemical shift data, coupling constants, and information obtained from substituted derivatives.

In almost all cases, for the determination of peak assignments, proton spectra were recorded in DMSO-d₆. In this solvent the resonances are better separated than in D₂O/DCI, and the substrates show greater solubility. The degree of long range coupling appeared to be reduced in DMSO, thus simplifying spectral interpretation a great deal.

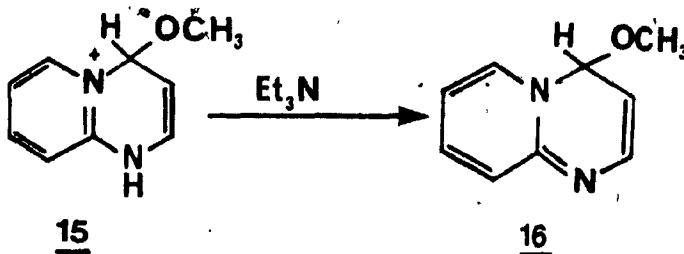
At 400 MHz, we were able to obtain many more coupling constants than at 60 MHz. The chemical shift assignments given by Sawyer and Wibberley¹ agree reasonably well with those obtained at 400 MHz, despite the different solvents used. Clearly, the superior resolution afforded by the high field instrument permitted much greater separation of chemical shifts. For example, at 60 MHz the hydrogens at positions 2 and 4, are not resolvable, neither are the 3H and 7H protons. At 400 MHz in DMSO, however, all resonances are well resolved and separated. Similar improvements in the spectra of the substituted derivatives of PP+ were also observed.

*
The NMR spectrum of the ring-opened compound PA was

also recorded. Not surprisingly, PA is trans about the carbon-carbon double bond, in both DMSO and D_2O/DCI , as indicated by the large coupling constant of 12 Hz between the vinylic hydrogens. In $CDCl_3$ however, PA exists as a ca. 3:1 mixture of the cis and trans isomers, respectively. This is attributed to intramolecular hydrogen bonding of the cis form in the aprotic chloroform, as shown in 14.¹

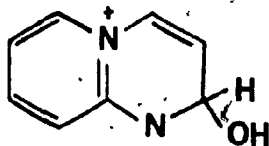
14

We corroborate here the NMR data of Tamura and Ono⁴ with respect to a ca. 1:1 mixture of 4H-4-deuteromethoxy pyrido-[1,2a]-pyrimidinium deuteriodide 15 and PP+ on taking an NMR of PP+ in perdeuteromethanol. Evidence of this mixture in methanol is also readily observable by UV. On adding triethylamine to the above, Tamura and Ono observed only the signals of 4H-4-deuteromethoxy pyrido-[1,2a]-pyrimidine 16.⁴

1516

We were able to observe the corresponding hydroxy analogue PBH+,* which is the protonated pseudobase of PP+, both transiently and at equilibrium. On dissolving crystals of PA in a D_2O solution of ca. pH 3 (chloroacetate buffer), signals due to PBH+ were observed. With time, these peaks disappeared, leading to formation of PP+ (Figure 3). These NMR spectra suggest a slow acid-catalysed elimination of water from the protonated pseudobase PBH+ to yield the stable cation PP+. This process, as well as observation of PBH+, is supported by UV spectral evidence given later in this thesis.

In a sample of PP+ in D_2O/DCI observed at 400 MHz (left for 14 hours to reach equilibrium), we were able to observe ca. 5% of the protonated pseudobase PBH+, as well as ca. 2% of what we assign tentatively to be the covalent hydrate of PP+ at position 2, 17 (see Figure 4).



17

The 7-bromo derivative of PP+ was also found to be in equilibrium with some of its covalent hydrate, 7-Br-PBH+.

*It is important to note that PBH+, the nitrogen protonated form of the pseudobase of PP+, is also considered to be a covalent hydrate of the parent compound.^{50,51,52}

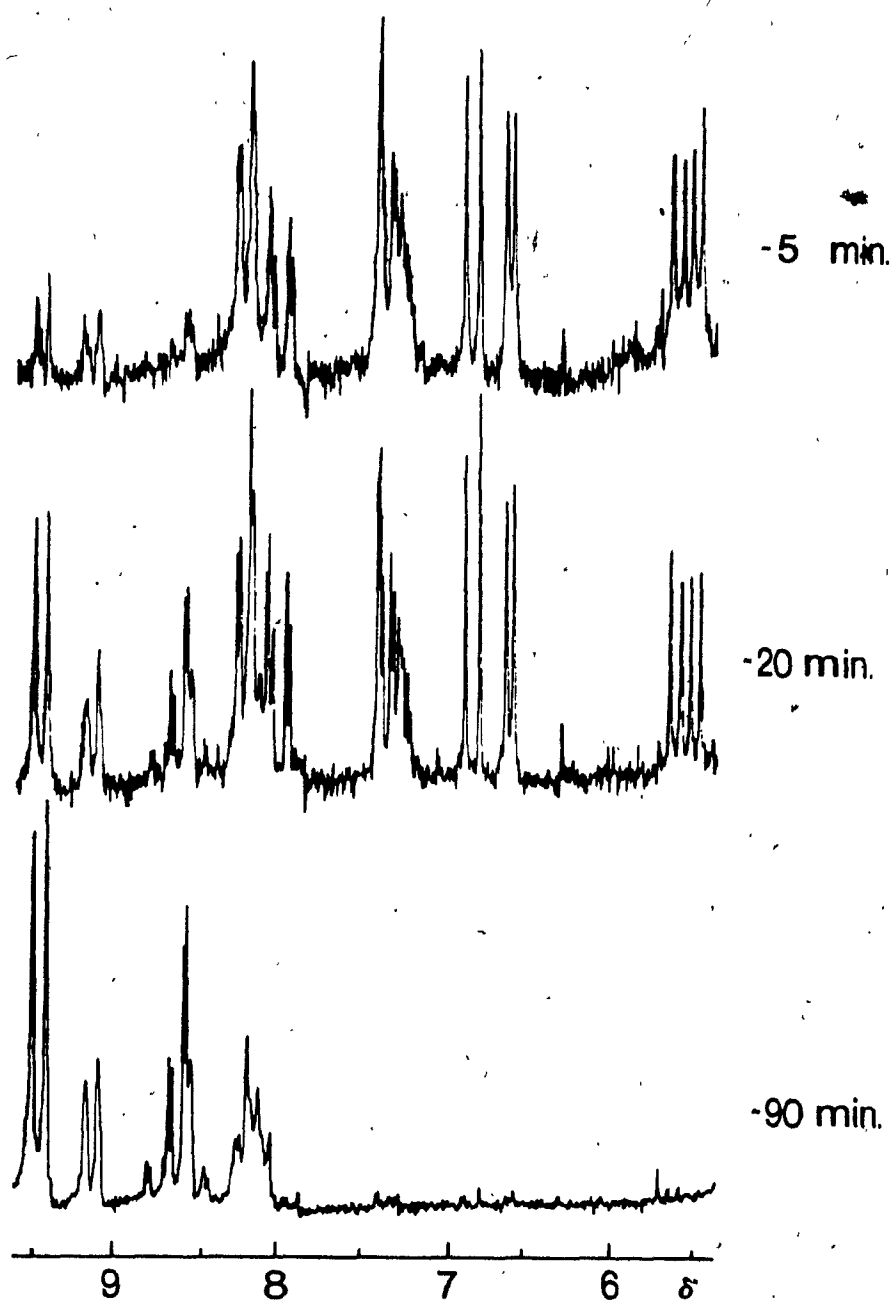


Figure 3. Dynamic NMR Spectra of $\text{PBH}^+ \rightleftharpoons \text{PP}^+$

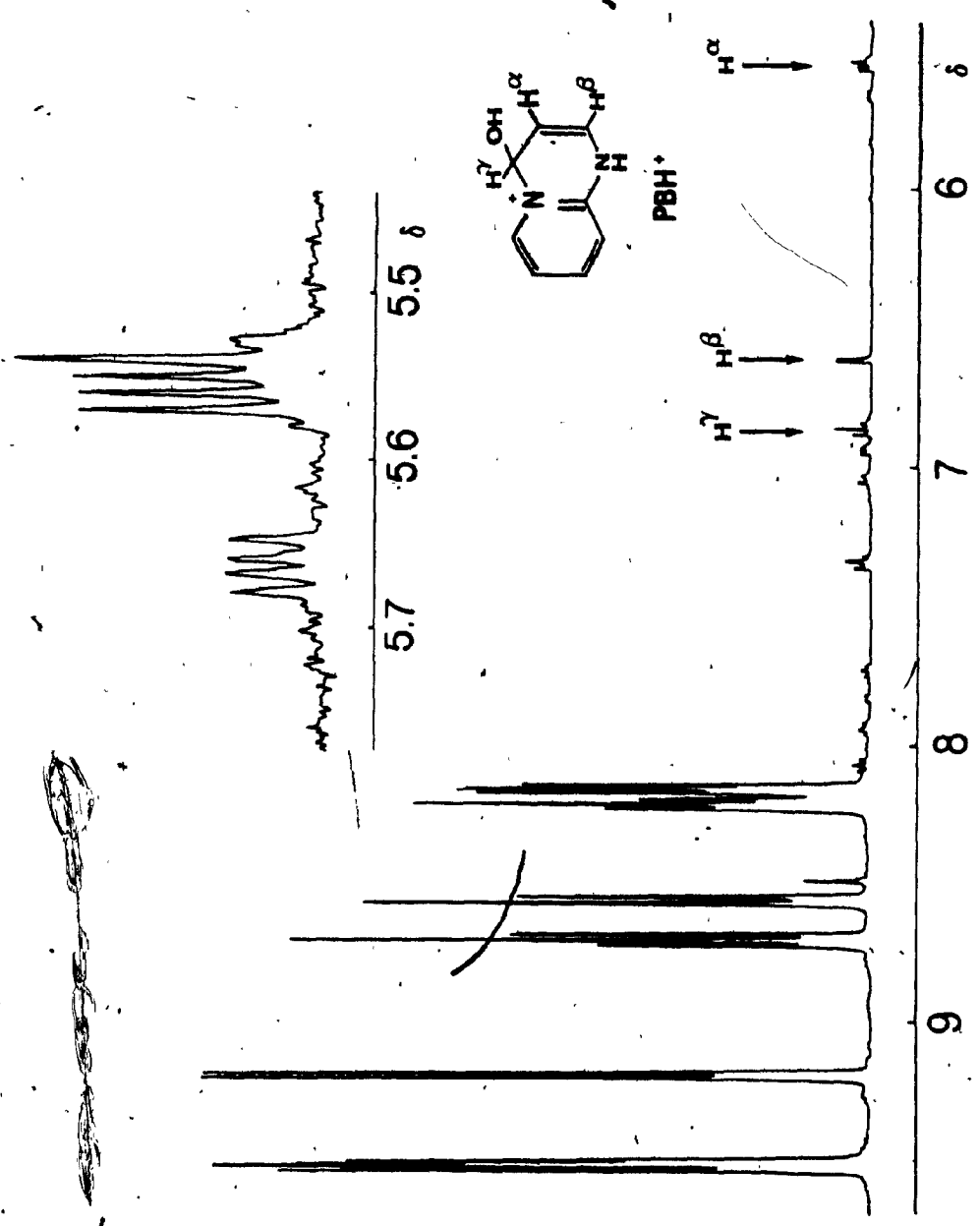


Figure 4. 400 MHz NMR Spectrum of PP+ in D₂O/DCI with 5% PBH+ present. Inset - α protons for 2 PBH+ and 17 (see text)

Table 8. Species observed by NMR at 400 MHz

Compound	H _α	H _γ	H _β	J _{α,β} (Hz)	J _{α,γ}	K _{eq} ^a
(15) ^b	5.49	7.02	6.63	8.0	4.2	ca. 2 ^c
PBH+ ^d	5.54	6.85	6.58	8.3	4.2	0.056
PBH+ ^e	5.55	6.87	6.61	8.2	4.4	0.056
BrPBH+ ^e	5.57	6.85	6.55	8.0	4.0	0.064
(17) ^e	5.66	f	f	8.2	4.4	ca. 0.02

^aK_{eq} = [cmpd.]/[PP+]

^bObserved at 80 MHz in methanol -- calibrated on solvent signal.

^cbased on 1:1.4 mixture observed by Tamura and Ono.⁴

^dObserved at 80 MHz in D₂O/DCI -- calibrated with DSS.

^eObserved at 400 MHz in D₂O/DCI -- calibrated with DSS.

^fnot observed

Only one species of protonated pseudobase was observed in this instance. No covalent hydration was observed for any of the methylated derivatives studied. This is presumably due to both electronic and steric effects of the methyls. The 2- and 4- methyl groups should stabilise the unhydrated cation more than its hydrate and a methyl at position 4 should hinder attachment of hydroxyl at that position.⁵⁰

Chemical shift data for the protonated pseudobases observed are given in Table 8, as well as equilibrium constants determined by NMR (400 MHz) for the above equilibria.

2. UV Spectra

Table 9 gives the UV spectra of PP+ and several of its derivatives under various conditions of pH. UV scans of PP+ and PA are illustrated in Figure 5, and show significant differences in the spectra of the cation and its ring-opened amino-carbonyl form.

We prepared PA⁴ and its UV spectrum matched that of PA generated in situ at pH 11 from PP+. On acidifying this solution, the spectrum of PP+ was regenerated. At higher pH (pH 14), the spectrum of PA undergoes a bathochromic shift, corresponding to ionisation to PA-, which then slowly hydrolyses to 2-aminopyridine and

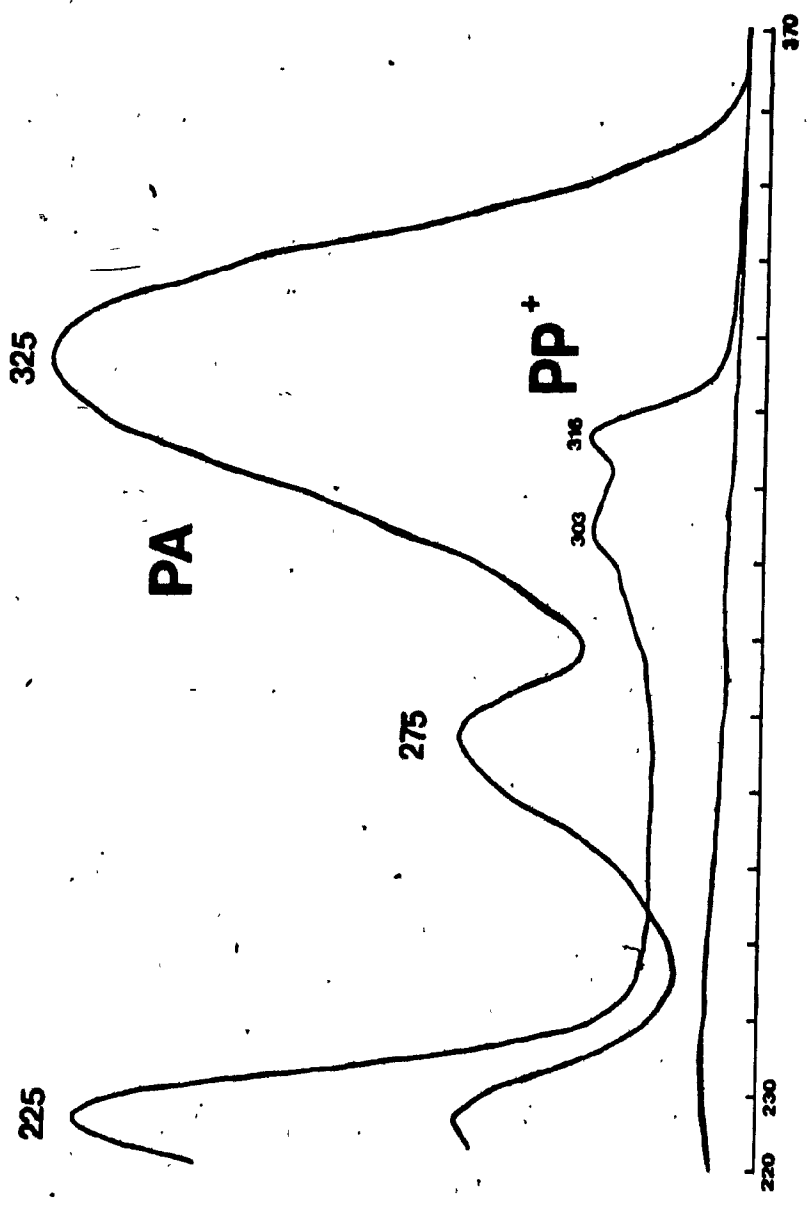


Figure 5. Static UV Spectra of PP+ and PA in Aqueous solution

Table 9. Static UV Spectra in Aqueous Solution.^a

Parent Species	pH	λ_{\max} nm. (log ϵ)
<u>PP+</u>	2	316(3.75), 303(3.71) 225(4.43)
	11	324br (4.60), 270(4.24), 204(4.08)
	14 ^b	ca. 343br (4.4), ca. 289br, sh (4.06), large end abs. 200 to 220 nm.
<u>MPP+</u>	2	317(3.81), 311(3.71), 305(3.74), 225(4.48), 206(4.32)
	12 ^c	334br (4.49), 281(4.01), 205(4.54)
	14 ^b	ca. 361 (4.37), ca. 290br sh (3.92), large end abs. 200 to 220 nm.
<u>DMPP+</u>	2	315(3.83), 309(3.70), 302(3.77), 227(4.55), 207(4.35)
	12 ^c	332br (4.35), 223sh (3.83), 206(4.55)
	14 ^b	ca. 329vbr (4.27), large end abs 200 to 220 nm.
<u>7-BrPP+</u>	2	323(3.74), 314sh (3.72), 310(3.75), 232(4.43)
	12	336br (4.54), 287(4.18), 205(4.54)
	14 ^b	ca. 354br (4.43), ca. 304 (4.12)

^a sh = shoulder, br = broad, v br = very broad.

^b Wavelengths and extinction coefficients are approximate due to slow hydrolysis of the ring opened aldehyde.

^c Spectra of ring-opened compounds were taken after sufficient time for ring-opening to occur.

the conjugate base of malondialdehyde (Figure 6). This interpretation is supported by hydrolysing malondialdehyde bis-(dimethyl acetal) in dilute HCl to give malondialdehyde, and subsequently ionising the dialdehyde to its conjugate base at high pH. Tamura and Ono⁴ have also reported direct evidence for these processes, by both NMR and UV methods. From the observed ionisation of PA to PA⁻, we estimate this pK_a to be approximately 13.5, at 25°C and 1.0 M ionic strength.

UV spectral scans support the above, with PP⁺ in acid mixed (1:1) with a solution of pH 7, slowly yielding the spectrum of PA (Figure 7). PA generated in situ (pH 11) slowly gives the spectrum of the cation PP⁺ on rendering the solution acidic and this is consistent with the dynamic NMR experiments (Figure 3) reported earlier.

PBH⁺ was observed by UV spectroscopy by mixing 10^{-4} M PA with a dilute HCl solution of pH ca. 1.5. The resultant solution was immediately scanned at 20 nm/sec. The spectrum of PBH⁺ is given in Figure 8, with peak positions and extinction coefficients listed in Table 10. This spectrum is similar to that obtained by Tamura and Ono⁴ for the corresponding methoxy compound 15. With time, the spectrum of the product PP⁺ appears.

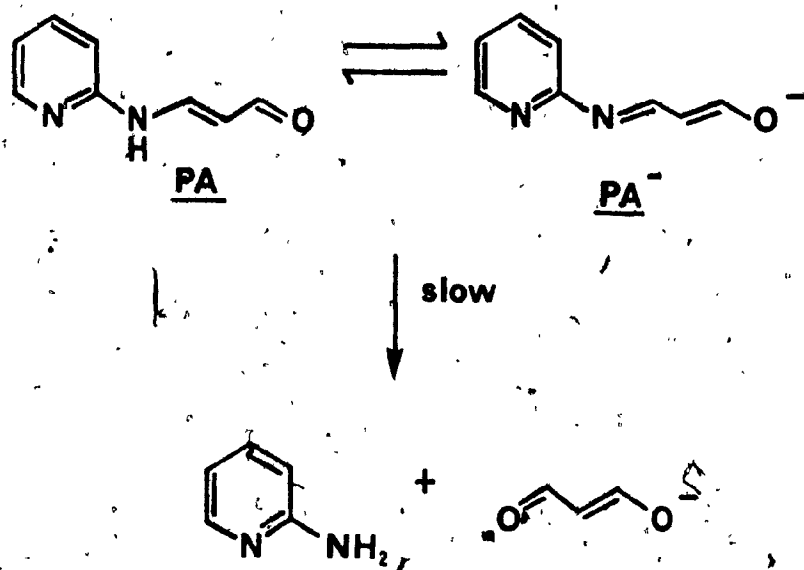
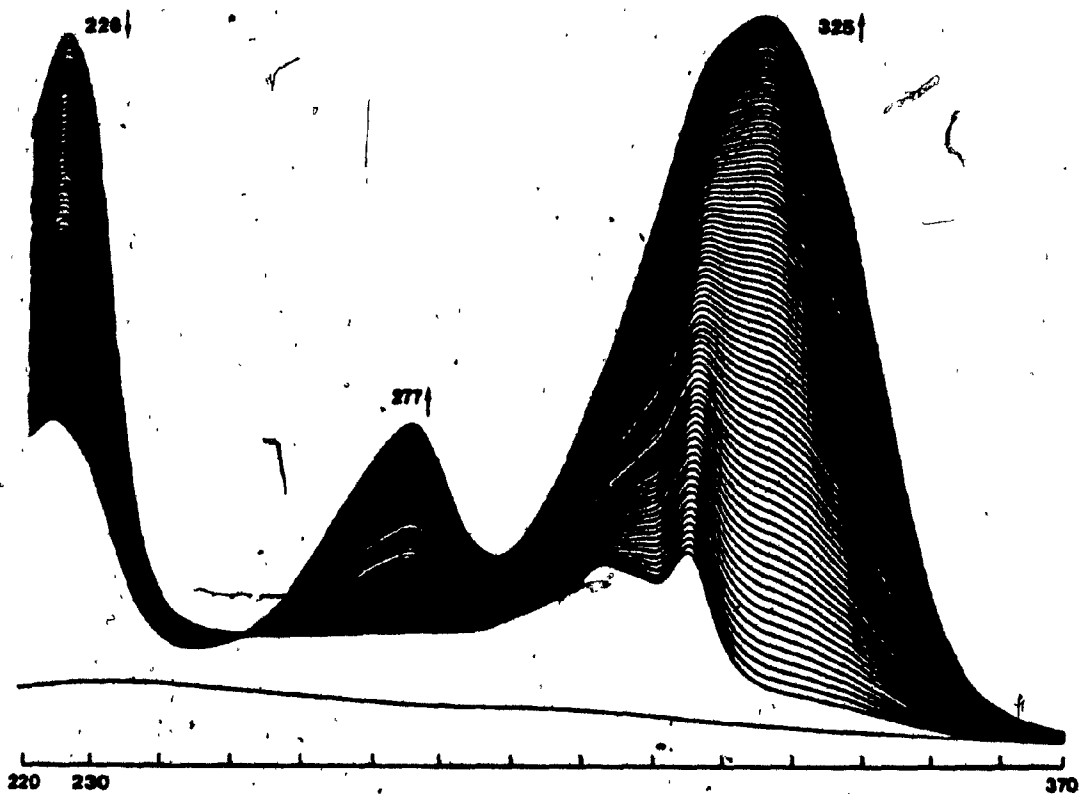


Figure 6. Slow hydrolysis of PA at high pH.



process b

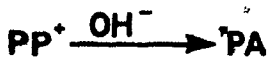


Figure 7. UV spectral scans at pH 7.

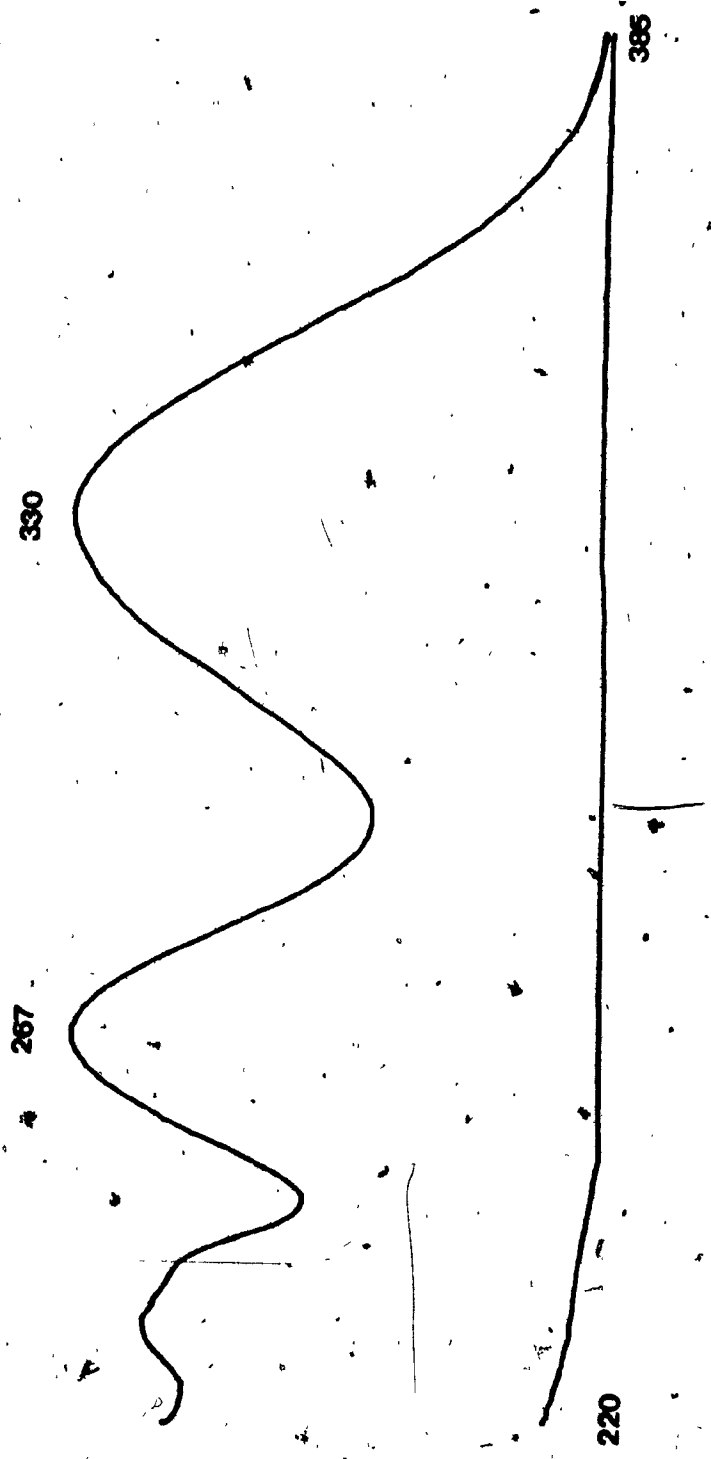


Figure 8. UV Spectrum of PBH^+ in H_2O , ca. pH 2

Table 10. UV Spectral data for PBH+

λ_{\max}	$\log \epsilon$
232 (239, sh)	3.67
267, br	3.76
328, br	3.76

The apparent pK_a between PP+ and PA, at 1M ionic strength (25°C) was determined spectrophotometrically by the method of Albert and Serjeant⁴¹ to be 5.90, at 25°C and $\mu = 1.0M$. This marks the bottom of the "well" on the pH-rate profile of PP+ (Figure 9). Table 11 contains equilibrium constants calculated or estimated for this study.

Using an authentic sample of PA, kinetically determined rates corresponding to ring-closing were identical to those obtained with a sample of PA generated in situ, within experimental error, for both the fast and the slow processes.

KINETIC RESULTS

All reactions were carried out under pseudo-first order conditions (see Experimental section) and the kinetic data obtained is presented in the form of pH-rate

profiles (see Figures 9-11). For the parent PP+, the pH-rate profile corresponding to PP+ \rightleftharpoons PA contains four separate regions, labelled (a) through (d). Rate profiles for the substituted derivatives studied are referred to, where appropriate.

Reactions corresponding to ring-opening of PP+ to PA are examined first, with the ring-closing processes being analysed later.

Process (a)

This reaction involves the base-catalysed ring-opening of PBH+ to PA. Initially, this process was observed by mixing a solution of PP+ with buffers of pH 5 - 8.5 in the stopped flow, and observing a small (<0.05 absorbance units) absorbance increase at 325nm (PA maximum). Due to this small absorbance change, it was not possible to ascertain the product of this reaction, as the product (PA) from the slow ring-closing process (b) interfered. From the NMR experiments it was noticed that ca. 5% of the protonated pseudobase PBH+ was observed to exist in equilibrium with PP+ and the small absorbance change observed seemed to correlate with the reaction of this species. This proposal was tested as follows:

PBH+ was generated in solution (see NMR section) and was subsequently reacted with buffers of pH 5 - 9.5 in the stopped flow. That is, a solution of 10^{-4} M

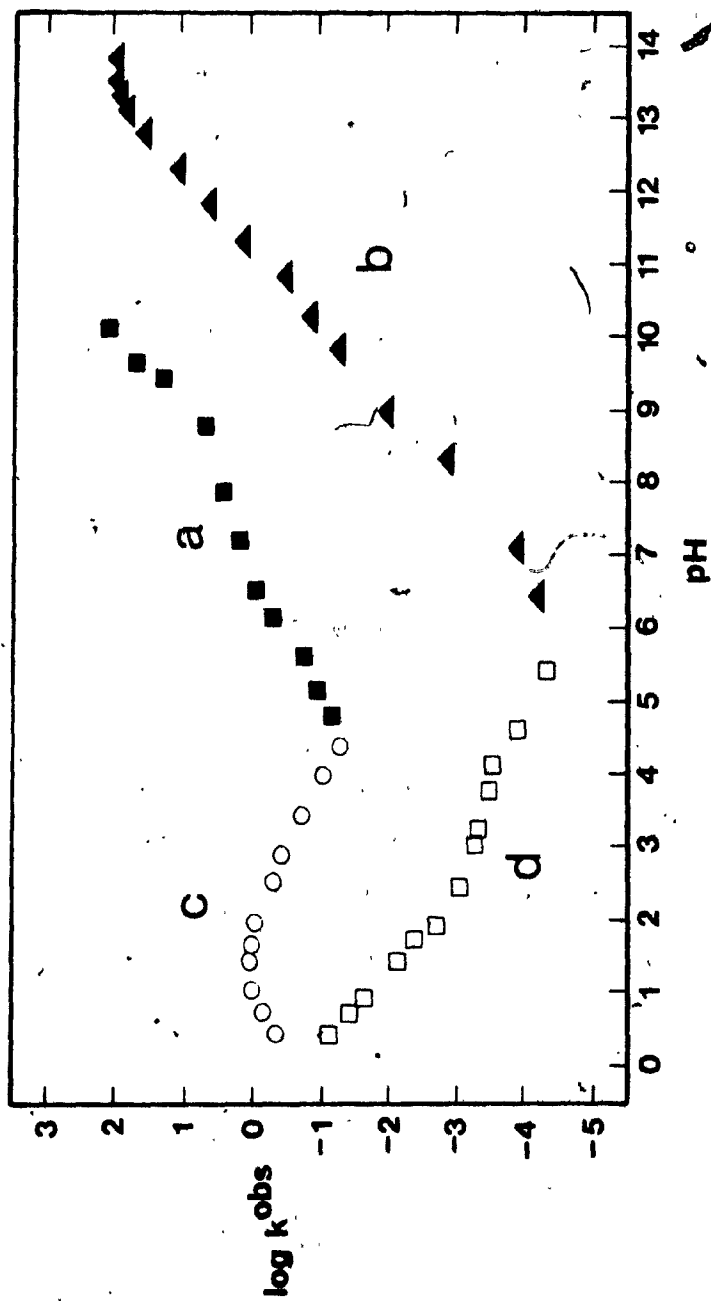
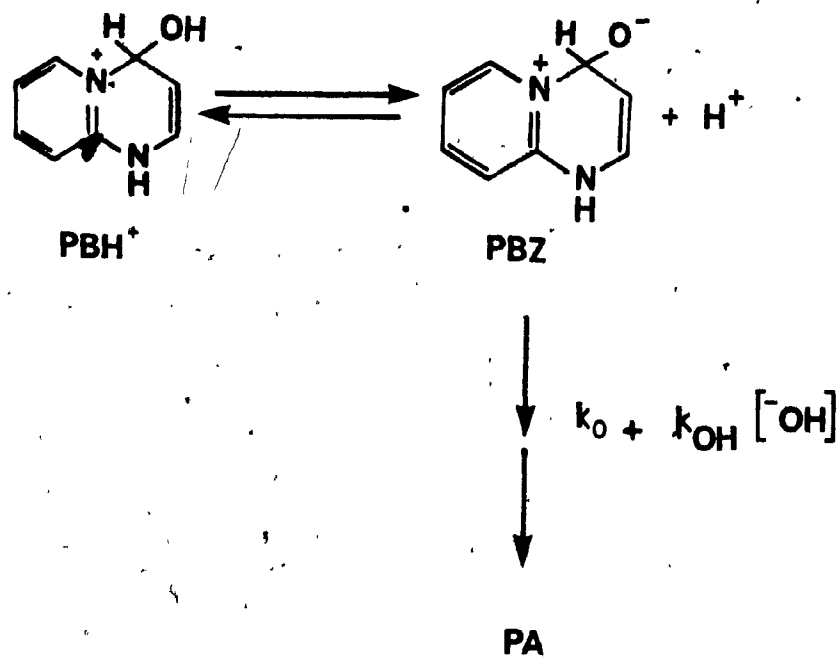


Figure 9. pH-rate profile for $\text{PP}^+ \rightleftharpoons \text{PA}$



Scheme 7. Proposed mechanism for the conversion of PBH⁺ to PA

PA was mixed 1:1 with 10^{-3} M HCl. PBH+ so prepared was rapidly reacted with buffers of appropriate pH in the stopped-flow. From the dynamic NMR spectra recorded previously (vide supra) it was observed that in acidic solution, PBH+ undergoes slow acid-catalysed dehydration to yield PP+ (process (d)). The slow rate of this dehydration allowed us to generate PBH+ in situ and subsequently study its reactivity in more basic solution. Using PBH+ prepared in this manner, the product of process (a) was ascertained to be PA. Rate constants obtained in this manner were identical to those obtained with PP+, within experimental error. From these experiments, this reaction involves the base catalysed conversion of PBH+ to PA.

The stepped shape of the rate profile for process (a) can be explained by Scheme 7. The following equation was derived to describe this behavior:

$$k^{\text{obs}} = \frac{(k_0[\text{H}^+] + k_{\text{OH}}K_4)K_4}{(K_4 + [\text{H}^+])[\text{H}^+]} \quad (19)$$

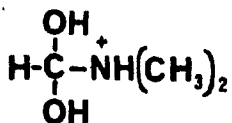
$$\text{where } k_0 = 1.54 \text{ s}^{-1}$$

$$k_{\text{OH}} = 7.72 \times 10^{-5} \text{ M}^{-1}\text{s}^{-1}$$

$$K_4 = 2.57 \times 10^{-7} \text{ M}$$

$$\text{p}K_4 = 6.59$$

These rate constants were calculated using the PROFIT programme on an Apple II microcomputer. This equation takes into account the three regions observed by ascribing the levelling off at pH 6.59 to be the pK_a between PBH^+ and its zwitterion PBZ . PBH^+ is in equilibrium with its zwitterion PBZ , which reacts by both a base catalysed and an uncatalysed pathway to yield PA . The pK_a of 6.59 (25°C, $I = 1$) is of the same order as those given by Guthrie⁵³ for similar compounds such as:



$pK_a = 7.8$ for dissociation of OH.

Process (b)

This process involved monitoring the ring-opening of PP^+ in basic solution to yield PA . That is, an increase in the absorbance due to PA was followed. A series of spectral scans (Figure 7) performed at pH 7 revealed no intermediates in this process, with only an increase in absorbance of the ring-opened compound being observed. Likewise, no intermediates were

Table 11. Equilibrium Constants

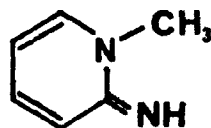
Equilibrium	K_{eq}
$\underline{PP+} + H_2O \rightleftharpoons \underline{PA} + H+$	$K_1 = [PA][H+]/[PP+] = 10^{-5.9M^a}$
$\underline{PP+} \rightleftharpoons \underline{PBH+}$	$K_2 = [PBH+]/[PP+] = 0.056^a$
$\underline{PBH+} \rightleftharpoons \underline{PA} + H+$	$K_3 = [PA][H+]/[PBH+] = K_1/K_2$ $= 10^{-4.62M^b}$
$\underline{PBH+} \rightleftharpoons \underline{PBZ} + H+$	$K_4 = [PBZ][H+]/[PBH+] = 10^{-6.59M^c}$
$\underline{PBH+} \rightleftharpoons \underline{PB} + H+$	$K_5 = [PB][H+]/[PBH+] = 10^{-12.5M^d}$
$\underline{PBZ} \rightleftharpoons \underline{PB}$	$K_6 = [PB]/[PBZ] = K_5/K_4 = 10^{-5.9M}$
$\underline{PP+} + H_2O \rightleftharpoons \underline{PB} + H+$	$K_{R+} = [PB][H+]/[PP+] \text{ (see page 67)}$

^ameasured at equilibrium

^bcalculated

^cmeasured from kinetics

^destimated from pK_a of



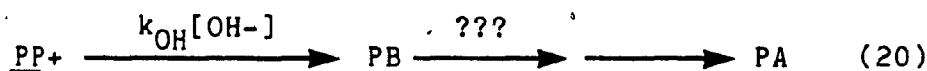
= 13.02

(reference: M.J. Cook, A.R. Katritzky, P. Linda, R.D. Tack, J.C.S. Perkin Trans. 2, 1295 (1972))

observed during the course of NMR studies performed.

For PP+, 7-BrPP+, MPP+, and DMPP+, a monotonic increase in log rate was observed with pH (Figure 10). The rate profiles of PP+ and its 7-bromo derivative, however, level off at high pH, indicative of either a pK_a or a change of rate-limiting step.

We attribute the monotonic rate increase with $[OH^-]$ to a hydroxide ion catalysed reaction on PP+, presumably forming the pseudobase PB, which then goes on to give the product PA.



Values of k_{OH} for the compounds examined are given in Table 12.

Table 12. k_{OH} values for PP+ \rightarrow PA (process (b))

Compound	$k_{OH}, M^{-1}s^{-1}$
<u>PP+</u>	496
<u>7-BrPP+</u>	1493
<u>4-MePP+</u>	6.81
<u>2,4-diMePP+</u>	1.01

At this time we are unable to explain the levelling-

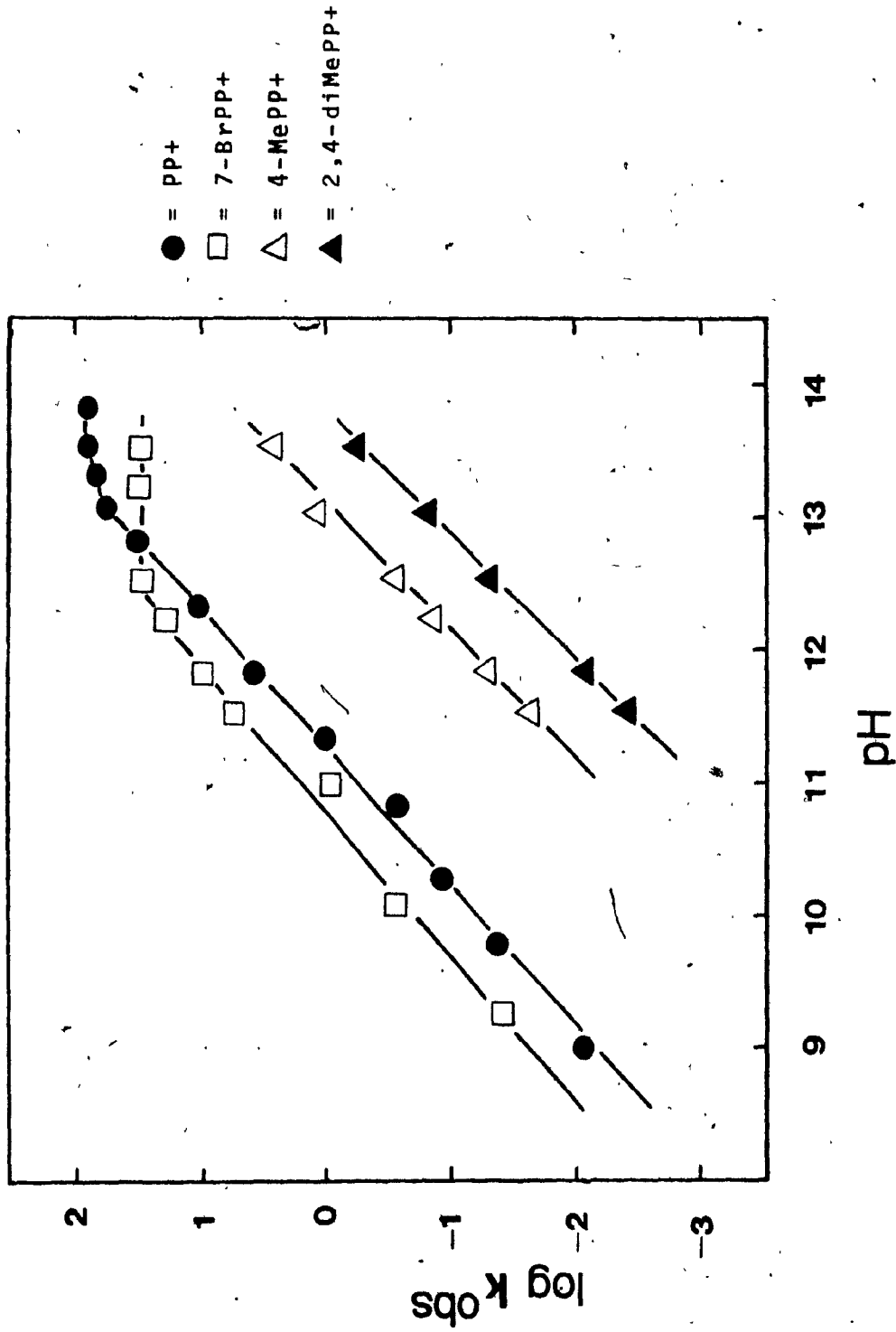
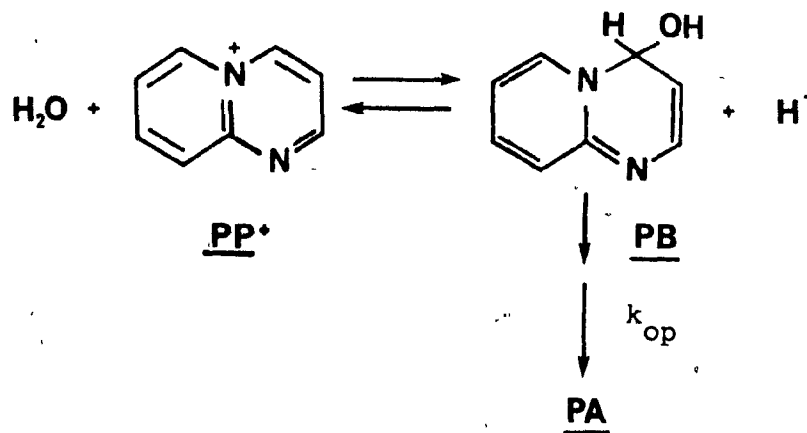


Figure 10. pH-rate profile for process b.

off of rate at high pH for PP+ and 7-Br-PP+ in a manner consistent with the mechanism proposed for process (a). As stated earlier, the levelling-off is due to either a pK_a or a change of rate-limiting step. Several proposed mechanisms are outlined below, along with reasons as to why they do not explain the experimental results.

Recall from process (a) that above ca. pH 9, the rate of reaction is observed to increase monotonically with pH to beyond the detection limit of the stopped-flow. This rules out reaction of process (b) by the mechanism proposed for (a), that is, via a hydroxide ion catalysed reaction on the zwitterion PBZ to yield PA.

If the rate plateau is assigned to a pK_a between PP+ and PB, the following is obtained. This gives



$$k^{obs} = \frac{k_{op} K_{R+}}{(k_{op} + [H^+])} \quad (21)$$

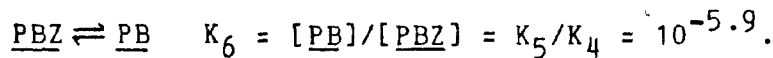
where $K_{R+} = \frac{[PB][H^+]}{[PP+]}$, and k_{op} is the rate

constant for ring opening. This corresponds to the plateau rate observed. Using the PROFIT programme, these constants were calculated and are presented below:

compound	K_{R+}, M	pK_{R+}	k_{op}, s^{-1}
<u>PP+</u>	4.46×10^{-14}	13.4	119
<u>7-BrPP+</u>	4.72×10^{-13}	12.3	37.4

Combining this proposal with the mechanism given for process (a) in Scheme 7 leads to the following:

If we assume that $K_{R+} = 10^{-13.4} M$ (the observed " pK_a ") then the equilibrium between PBZ and PB (see Table 10) is:

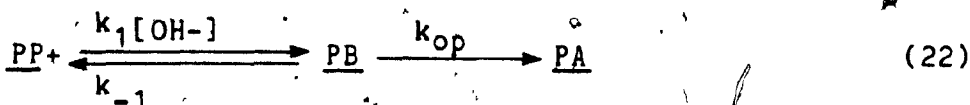


The value of K_6 of $10^{-5.9}$ indicated that only one in $10^{5.9}$ molecules exists as PB. The rest are in the form of PBZ, which contains an aromatic ring. This large equilibrium constant in favour of the zwitterion, as well as the value of k_{OH} of $7.72 \times 10^5 M^{-1} s^{-1}$ for hydroxide ion catalysis on PBZ, makes the proposal given in Scheme 7 highly unlikely. Base catalysed reaction via PBZ is clearly favoured, especially at the pHs in question.

Assuming a pK_a between the pseudobase PB and its anion PB- was also considered to account for the levelling

off observed. This proposal was rejected as it requires two moles of OH⁻ for each mole of substrate, while the rate profile indicates that only one OH⁻ is involved.

A change of rate-determining step is another possible explanation for the flattening-out observed. If we assume a model as in equation 22,



we can invoke a steady state approximation on PB, as no intermediates were spectrally observed. This gives

$$k^{\text{obs}} = k_{\text{OH}}[\text{OH}^-]k_{\text{op}}(k_{-1} + k_{\text{op}}) \quad (23)$$

Two extreme cases exist here:

Case (i) if $k_{\text{op}} \gg k_{-1}$, then $k^{\text{obs}} = k_{\text{OH}}[\text{OH}^-]$.

This accounts for the monotonic increase of k^{obs} with pH.

Case (ii) if $k_{\text{op}} \ll k_{-1}$, then $k^{\text{obs}} = k_{\text{op}}k_{\text{OH}}[\text{OH}^-]/k_{-1}$, or $k^{\text{obs}} = k'[\text{OH}^-]$. This rate expression is also [OH⁻] dependent and is kinetically indistinguishable from that given in case (i). Obviously, a mechanism involving a change of rate-limiting step of the type shown in equation 22 cannot account for the observed results since both k_{op} and k_{-1} are pH independent.

We are therefore not able to interpret the levelling-off of the rate profile in a manner consistent with the

mechanism given for process (a) at this time. We can say, however, that an OH- catalysed step of the general form outlined in equation 20 is occurring. This type of reaction is supported by the results obtained from ring-opening experiments performed with several substituted derivatives of PP^+ .

The two methyl substituted derivatives studied also undergo ring opening to their corresponding amino-carbonyl compounds, but at a slower rate than for PP^+ , as shown in Figure 10. Values of k_{OH} are given in Table 11. The relative magnitudes of k_{OH} observed can be accounted for in several ways. The presence of methyl substituents on the parent compound acts to reduce the rate of ring-opening and subsequent cis-trans isomerisation of the product. Both involve movement of heavy atoms and hence a rate reduction for the substituted compounds is expected. Another factor to be considered is steric hindrance at the 4-position caused by the presence of a methyl group. Attack of OH- should occur more slowly on the methylated derivatives, due to steric interference.¹³ Stabilisation of the parent cation by the methyl groups present is another possible explanation for the decrease in rate observed.¹³ The substituent(s) can further delocalise the positive charge in the parent PP^+ , thus rendering it more stable and hence less susceptible to nucleophilic attack by hydroxide ion. The somewhat faster

reaction rate of 7-BrPP+ probably reflects, to an extent, the inductive electron withdrawing effect of the bromo substituent on the stabilisation of PP+. These explanations are all consistent with equation 20 and support this type of reaction.

Process (c)

From the NMR studies outlined previously, this process was found to involve conversion of PA to PBH+. The protonated pseudobase subsequently undergoes slow dehydration to give PP+ in process (d).

The pH-rate profile for processes (a) and (c) exhibit a "well" at pH 4.6, corresponding to an equilibration of PBH+ with PA. This statement is affirmed by spectral studies and is consistent with other measurements. From NMR studies $K_2 = [\text{PBH}^+]/[\text{PP}^+] = 0.056$ and from UV measurements $K_1 = [\text{PA}][\text{H}^+]/[\text{PP}^+] = 10^{-5.90} \text{ M}$ (see Table 11). Accordingly, $K_3 = [\text{PA}][\text{H}^+]/[\text{PBH}^+] = K_1/K_2 = 10^{-4.62} \text{ M}$, in good agreement with the minimum in the rate-profiles for processes (a) and (c). $\text{p}K_3 = 4.62$ is also reflected in process (d), which is discussed later.

Process (c) shows (general) acid catalysis above pH 2 and is independent of $[\text{H}^+]$ below this point. The changeover is due to a change of rate-limiting step, rather than a $\text{p}K_a$, and this is borne out by buffer catalysis

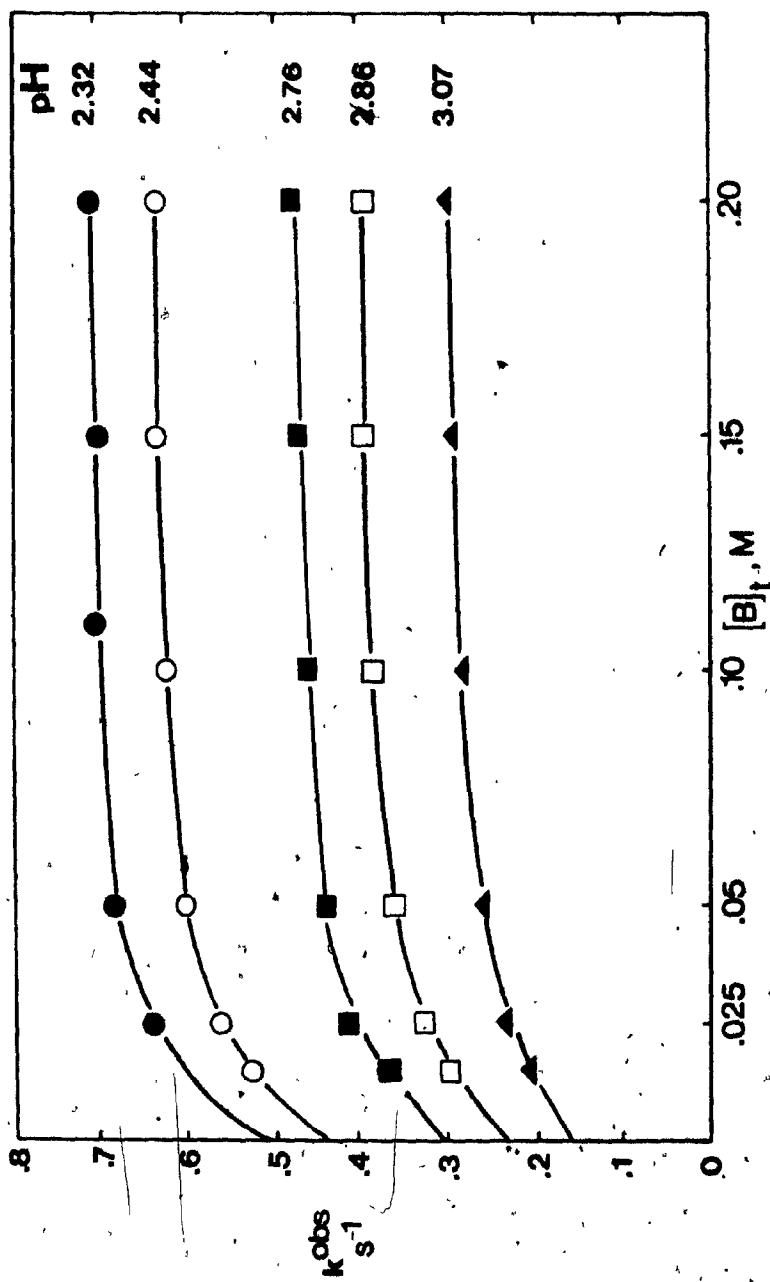
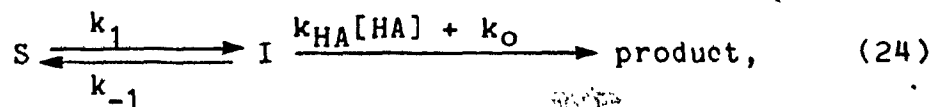


Figure 11. Buffer catalysis plots for process (c) - chloroacetate buffers.

studies performed. The 7-bromo derivative of PP+ was found to react in a similar manner to PP+, but the "well" appears to be shifted to approximately pH 2.5 and the levelling off corresponding to a change in rate-limiting step is observed at lower pH (ca. 1.5). The inductive electron-withdrawing effect of the bromo substituent destabilises PBH+ and so lowers the pK_a of PBH+ \rightleftharpoons PA + H^+ .

4-Me-PP+ also exhibited some reactivity in this region, but as the absorbance changes were found to be very small, this compound was not further investigated.

Buffer catalysis was observed for PA \rightleftharpoons PBH+ in the range of pH 2 to 4.5 (cyanoacetate, chloroacetate, formate, β -chloropropionate and acetate buffers). Curved plots of k^{obs} versus [buffer], showing levelling-off at high buffer were obtained through this range. Sample plots of chloroacetate buffer catalysis are presented in Figure 11. These curved plots lend support to a change of rate-determining step with increasing acidity. The simplest model to account for this type of behavior is the following:



where k_0 contains a term in $[H^+]$, as the buffer plots have non-zero intercepts. Since no build-up of intermediates was observed for this process, a steady state

approximation can be used for [I], which gives:

$$k_{\text{obs}} = \frac{k_1(k_0 + k_{\text{HA}}[\text{HA}])}{(k_{-1} + k_0 + k_{\text{HA}}[\text{HA}])} \quad (25)$$

This equation accounts for the curved buffer plots observed and is valid only at a given pH, as k_0 contains a term in H^+ . At low buffer, the reaction is dependent on [HA], as the $k_{\text{HA}}[\text{HA}]$ term is rate limiting. At high [buffer], k_0 and k_{-1} are small relative to $k_{\text{HA}}[\text{HA}]$ and equation 25 reduces to

$$k_{\text{obs}} = k_1 = k_{\text{max}} \quad (26)$$

Equation 26 is independent of HA and so accounts for the levelling off of the buffer plots obtained at high [buffer]. Dividing the right-hand side of equation 25 through by k_{-1} gives:

$$k_{\text{obs}} = \frac{k_1(k_0' + k_{\text{HA}}'[\text{HA}])}{(1 + k_0' + k_{\text{HA}}'[\text{HA}])} \quad (27)$$

where a ' symbol denotes division by k_{-1} .

Analysis of buffer catalysis data obtained for chloroacetate buffers using an iterative non-linear regression programme (CURVBUF) gave the constants listed in Table 12.

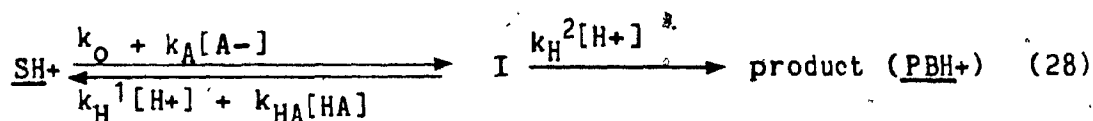
Table 13. Rate constants obtained for Buffer catalysis with CURVBUF programme (Process (c) - chloroacetate buffers)

pH	k_1	k_0'	k_{HA}'	$k_{\text{HA}}'/f_{\text{HA}}$
2.32	0.723	1.02	252	348

2.44	0.647	0.822	231	346
2.70	0.487	0.628	176	337
2.86	0.407	0.572	146	338
3.07	0.310	0.584	96.1	302
	(s ⁻¹)	(s ⁻¹)	(M ⁻¹ s ⁻¹)	(M ⁻¹ s ⁻¹)

Values of k_{HA} divided by f_{HA} (fraction of undissociated HA) are relatively constant throughout the pH range studied with this buffer and are much larger than k_0 and k_1 values. The rate constants k_1 and k_0 appear to decrease with pH to approximately the same degree. If process (c) were to follow the simple model outlined in equation 20, k_1 would be expected to be pH independent as it does not contain a term in $[H^+]$.

Another possible model, outlined in equation 28 was considered to account for the buffer catalysis observed. In the pH region of process (c), the substrate PA is expected to be protonated. If this is the case, then the rate profile reflects an acid catalysed reaction on a cation to yield the cation PBH⁺.



The pK_a for protonation (of the ring nitrogen) of a similar compound, N-acetyl-2-aminopyridine is 4.09.⁵¹

The added C=C moiety present in PA is expected to attenuate the electron withdrawing effect of the carbonyl

group somewhat and so a pK_a for protonation of around 4.5 is not unreasonable. A general base-catalysed (and uncatalysed) removal of the acidic proton from PAH^+ (= SH^+ , protonated substrate) to form the intermediate I is proposed (along with its microscopic reverse), with subsequent acid-catalysed conversion of I to give PBH^+ .

Using the steady state approximation on I gives

$$k^{\text{obs}} = \frac{(k_o + k_A[A^-])k_H^2[H^+]}{(k_H^2[H^+] + k_H^1[H^+] + k_{HA}[HA])} \quad (29)$$

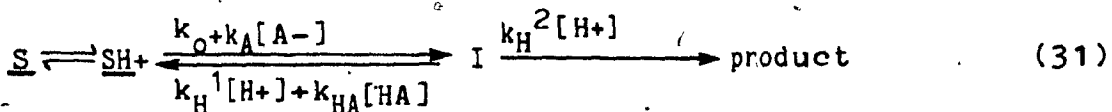
At zero buffer concentration, equation (29) reduces to

$$k^{\text{obs}} = k_o k_H^2 / (k_H^1 + k_H^2) \quad (30)$$

which is pH independent. This does not reflect the experimental results, as the intercept values of the buffer plots vary with $[H^+]$.

Similarly, for high buffer concentrations the appropriate simplified form of equation 29 does not account for the observed behavior.

Modifying equation 28 to reflect a pre-equilibrium protonation of the substrate gives



The expression for k^{obs} here is similar to equation 29, save for an initial multiplying factor of $[H^+] / ([H^+] + K_{\text{SH}^+})$, which reflects the fraction of molecules in the form SH^+ .

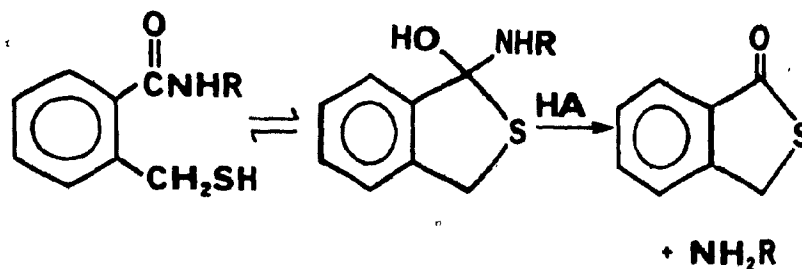
undergoing subsequent reaction.

$$k^{obs} = [H^+] / ([H^+] + K_{SH^+}) \times (\text{eqn. 29}) \quad (32)$$

If, as mentioned previously, the value of K_{SH^+} is approximately $10^{-4.5}$ M, then for the pH range over which process (c) extends, $[H^+] > K_{SH^+}$ and equation 32 reduces to equation 29. Therefore, this proposal fails to account for the experimental findings.

It is important to realise the limited range over which effective buffer catalysis experiments could be carried out for process (c). Since there is curvature around pH 2 and 4.6 (see Figure 9) useful buffer studies are only feasible between pH 3 - 3.6. Even in this region the rate profile does not attain a slope of -1, a necessary requirement for an acid catalysed reaction. This small region in which to carry out buffer catalysis experiments makes it difficult to perform a thorough analysis of process (c).

In summary, process (c) involves an acid catalysed conversion of PA to PBH⁺, which subsequently loses water to give PP⁺ in process (d). A change of rate-limiting step with increasing pH is indicated by both the rate profile and buffer catalysis studies. This type of behavior is indicative of a mechanism of the general type given in equation 24. Further support for this type of proposal is found in McDonald's work on the reaction:



The pH-rate profile obtained at acidic pHs for this reaction is similar to that for process (c) and curved buffer plots were obtained. This is interpreted as a change of rate-limiting step with pH, from the uncatalysed formation of the neutral tetrahedral intermediate at low pH, to its general acid-catalysed breakdown (or a kinetic equivalent) at higher pH.^{26b} In the present work a thorough analysis of buffer catalysis could not be performed due to the small pH region available for such studies. Protonation of the substrate PA in the pH region of process (c) also hindered a more definitive analysis of the mechanism of this reaction.

Process (d)

From the dynamic NMR spectra presented earlier, this process involves the acid-catalysed dehydration of PBH+ to give the stable cation PP+. The pH-rate profile shows

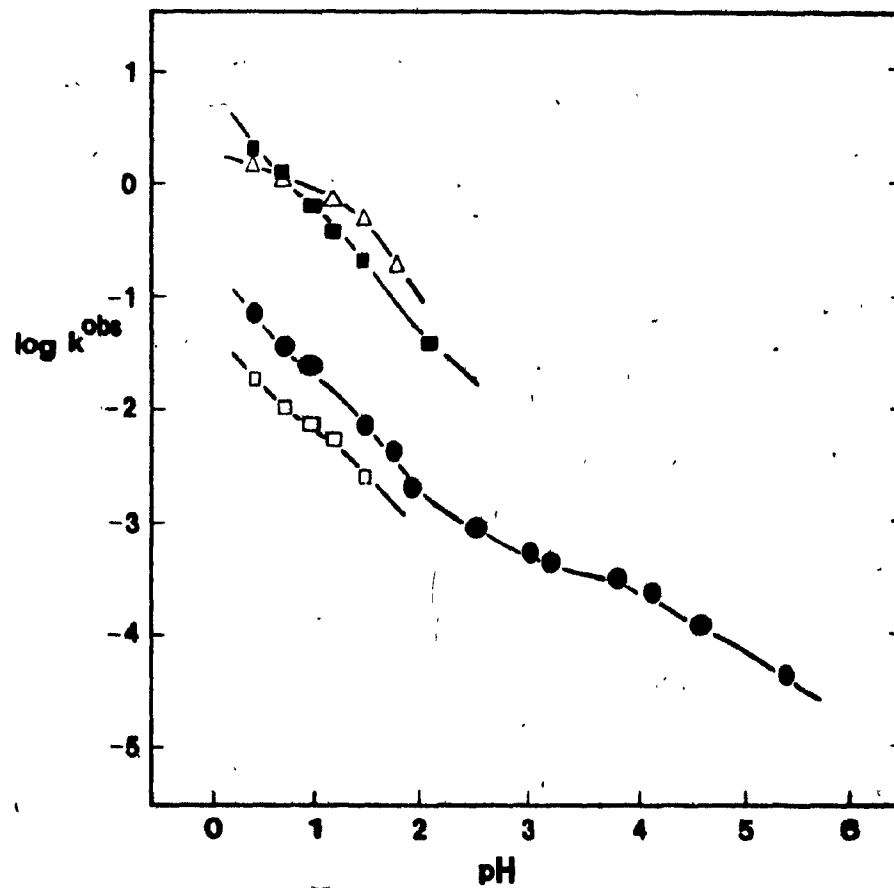


Figure 12. pH-rate profile for process (d)

● = PP+

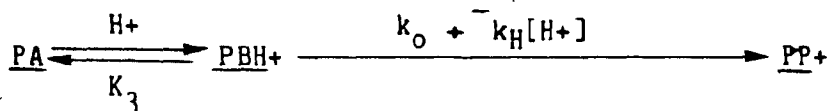
□ = MPP+ & 7-BrPP+ (process (d))

■ = DMPP+

Δ = 7-BrPP+ (process (c))

acid catalysis, save for a small region from ca. pH 3.5 to pH 4.6 where the rate is independent of acidity. The reaction is again H^+ catalysed below pH 4.6 to the bottom of the "well" at pH 5.90. This low point reflects the equilibration between PP^+ and PA .

The following equation accounts for the rate profile of process (d), with PBH^+ reacting via an acid-catalysed and an uncatalysed pathway.



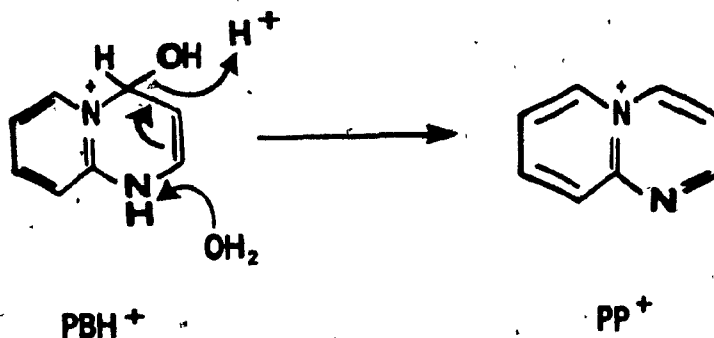
The levelling out is due to the apparent pK_a between PBH^+ and PA ($pK_3 = 4.62$).

General acid catalysis was observed for this process, but no in depth study was carried out. Acid catalysis on PBH^+ is proposed to occur via the mechanism overleaf. An alternative mechanism with a general acid HA delivering a proton and water abstracting the N-1 proton is also possible. However, we favour the proposal shown overleaf: Protonation of the hydroxy group by H_3O^+ ($pK_a = -1.74$) and abstraction of the proton on N-1 by a general base A- (e.g. chloroacetate ion, $pK_a = 2.70$). Energetically, this process is more feasible than protonation by HA (chloroacetic acid, say) and proton abstraction by H_2O ($pK_a = 15.74$).⁵⁴

Furthermore, the type of behavior proposed is seen in the enolisation of acetone. That is, specific acid

catalysed protonation of the carbonyl, with general base catalysed proton abstraction to yield the enol.⁵⁵

Substituted derivatives of PP^+ were also studied in this region (Figure 12). $2,4\text{-diMePP}^+$ reacts much faster than PP^+ , and this is due to the large stabilising effect of the two methyl substituents on the dehydration of $2,4\text{-diMePBH}^+$ to give $2,4\text{-diMePP}^+$. Interestingly, 4-MePBH^+ undergoes dehydration at a slower rate than PBH^+ . It appears that the methyl group at the 4 position reduces the amount of the covalent hydrate present, while having little effect on the rate of subsequent dehydration, relative to the unsubstituted compound. 7-BrPBH^+ loses water more slowly than PBH^+ , presumably due to the destabilising effect of the bromo substituent.



SUMMARY

The reversible ring-opening reaction of $\underline{PP+} \rightleftharpoons \underline{PA}$ involves two equilibrations: $\underline{PP+} \rightleftharpoons \underline{PA} + H^+$, $pK_a = 5.90$, and $\underline{PBH+} \rightleftharpoons \underline{PA} + H^+$, $pK_a = 4.62$. Both of these are shown on the pH-rate profile for $\underline{PP+} \rightleftharpoons \underline{PA}$. The protonated pseudobase of $\underline{PP+}$, $\underline{PBH+}$ was observed by both NMR and UV methods.

Four processes were found to occur for the reversible ring-opening of $\underline{PP+}$ to \underline{PA} . Process (a) involves ring opening of $\underline{PBH+}$ via OH^- catalysis and an uncatalysed pathway from the zwitterion, \underline{PBZ} . \underline{PBZ} is in equilibrium with the covalent hydrate of $\underline{PP+}$, where $pK_4 = 6.59$.

Process (b) involves ring-opening of $\underline{PP+}$ to \underline{PA} via rate-limiting hydroxide addition to $\underline{PP+}$, with subsequent ring opening to give \underline{PA} .

Process (c) is the acid-catalysed ring-closing of \underline{PA} to $\underline{PBH+}$, which then undergoes acid-catalysed dehydration to $\underline{PP+}$ in process (d).

Suggestions for further research include the following:

1. Examination of the kinetics and product(s) of the reaction of 2-aminopyridine and [malondialdehyde]. This type of study should shed light on the intermolecular condensation between these two species,

as opposed to the intramolecular condensation reaction to yield PBH^+ and PP^+ from PA .

2. Buffer catalysis experiments could be carried out on process (b) to aid in the interpretation of the levelling-off observed at high pH. A Brønsted plot could also be done to determine the β value and hence obtain further information regarding the mechanism of process (b).
3. A further study of the effects of substituents on the pyridine ring of PP^+ on the reaction $\text{PP}^+ \rightleftharpoons \text{PA}$ could be performed. That is, substituents ortho, meta and para to the quaternary nitrogen. Perhaps these substituted derivatives will give a better understanding of the $\text{PP}^+ \rightleftharpoons \text{PA}$ system.
4. Further study of the analogous reaction of the pyrimido-[1,2a]-pyrimidinium cation could be carried out to determine the effect of the added nitrogen in this symmetrical compound. Preliminary studies indicated that this compound undergoes ring-opening much faster than PP^+ and its ring-opened form undergoes ring-closure at a rate comparable to PP^+ .

REFERENCES

References

1. J.H.R. Sawyer and D.G. Wibberley, J.C.S. Perkin I, 1138, (1973).
2. V.A. Chuiguk and A.M. Khmaruk, Ukr. Khim. Zh., 41, 186, (1975) [CA 83, 9972 (1975)]
3. I. Hermez and Z. Meszaros, Adv. Het. Chem., 33, (1973) pp. 241-246, 290-291, and references cited therein.
4. S. Tamura and N. Ono, Chem. Pharm. Bull., 26 (10), 3162 (1978)
5. A.N. Nesmeyanov, M.I. Rybinskaya and N.K. Belskii, [CA 51, 14712 (1957)]
6. (i) O.S. Tee and M. Endo, Can. J. Chem., 54, 2681 (1976)
(ii) O.S. Tee and M. Endo, J. Het. Chem., 11, 441 (1974)
7. D.J. Brown, "The Pyrimidines", (Wiessberger Series), Wiley Interscience, (1962) pp. 31-72
8. L.A. Paquette, "Principles of Modern Heterocyclic Chemistry", W.A. Benjamin, New York (1968)
9. A.M. Khmaruk, Yu. M. Volovenko, V.A. Chuiguk, Ukr. Khim. Zh., 38, 262 (1972) [CA 76, 153698 (1972)]
10. V.A. Chuiguk and V.V. Oksanich, Khim. Geterotsikl. Soedin, 242 (1973) [CA 79, 6745 (1973)]
11. G.W. Fischer, German (East) Patent 113, 542 [CA 84, 105647 (1976)]
12. G.W. Fischer, Z. Chem., 18, 121 (1978)

[CA, 89, 23666 (1978)]

13. J.W. Bunting, Adv. Het. Chem., 25 (2) (1979), and references, cited therein.
14. W.P. Jencks, "Catalysis in Chemistry and Enzymology", McGraw-Hill, New York (1969)
15. M.L. Bender, "Mechanisms of Homogeneous Catalysis from Protons to Proteins", Wiley Interscience, New York (1971)
16. A. Fersht, "Enzyme Structure and Mechanism", W.H. Freeman and Co., Reading U.K. (1977)
17. D.R. Robinson, Tet. Lett., 5007, (1968)
D.R. Robinson, J. Am. Chem. Soc. 92, 3138 (1970)
18. B. Capon, A.K. Ghosh, D.M.A. Grieve, Acc. Chem. Res., 14, 306 (1981), and references cited therein.
19. O.S. Tee, R.A. McClelland, M. Trani, M.P. Jansen, The Kinetics and Mechanism of the Ring-Opening of the 1,3-dimethyl-5-oxo-pyrimidinium Cation, manuscript in preparation.
20. T.H. Lowry and K. Scheuller-Richardson, "Mechanism and Theory in Organic Chemistry", 2nd ed., Harper and Row, New York (1981), and references cited therein
21. H. Decker, J. Prakt Chem. [N.S.], 47, 28 (1893)
22. A. Hantzsch, Chem. Ber. 32, 575 (1899)
A. Hantzsch and M. Kalbe, ibid., 32, 3109 (1899)

23. J.W. Bunting and W.G. Meathrel, *Can. J. Chem.*, 50, 917 (1972)
24. W.P. Jencks, and J. Carruiolo, *J. Am. Chem. Soc.*, 83, 1743 (1961)
25. W.P. Jencks, *Acc. Chem. Res.*, 9, 425 (1976), and references cited therein.
26. see for example: (a) T. Okuyama, S. Kawao, T. Fueno, *J. Am. Chem. Soc.*, 105, 3320 (1983) (b) R.S. McDonald P. Patterson, A. Stevens-Whalley, *Can. J. Chem.*, 61, 1846 (1983)
27. E.F. Caldin, "Fast Reactions in Solution", J. Wiley and Sons Inc., London (1960),
28. Q.H. Gibson, *J. Physiol.* 117, 498 (1952)
Q.H. Gibson, *Faraday Soc.*, 17, 137 (1964)
Q.H. Gibson and C. Greenwood, *Biochem. J.*, 86, 541 (1963)
29. J.A. Sirs, *Trans. Faraday Soc.*, 54, 207 (1958)
J.A. Sirs, *ibid.*, 54, 201 (1958)
30. R.H. Prince, *ibid.*, 54, 838 (1958)
31. F.J.W. Roughton et al, *Proc. Roy. Soc. A*, 104, 376 (1923)
32. C.A. Fyfe, M. Cocivera and S.W.H. Damji, *Acc. Chem Res.*, 11, 277 (1978)
33. F.J.W. Roughton, "Investigations of Rates of Reactions

Part II" (Edited by Fries, Lewis and Wiessberger),
Wiley Interscience, New York (1963)

34. Empirically determined by R.S. McDonald, personal communication to O.S. Tee. This was verified in this laboratory.
35. D.D. Perrin and Boyd Dempsey, "Buffers for pH and Metal Ion Control", Chapman and Hall, London (1974)
Original Reference: Davies, J.C.S., 2093 (1938)
36. D.D. Perrin, Austr. J. Chem., 16, 572 (1963), see also reference no. 35
37. A.I. Vogel, "A Textbook of Quantitative Inorganic Analysis"; 2nd ed., Longmans, London (1951) pp. 31
38. H. Gilbert and W.P. Jencks, J. Am. Chem. Soc., 99, 7931 (1977)

39. G.D. Fasman, ed., "CRC Handbook of Biochemistry and Molecular Biology", 3rd ed., Vol. 1, CRC Press, Cleveland, Ohio (1976)
40. J. Sawyer and W.P. Jencks, J. Am. Chem. Soc., 99, 464 (1977)
41. A. Albert and E.P. Serjeant, "The Determination of Ionisation Constants", Methuen, London (1962)
42. J.J. Morrow, Chem. Instrumen., 3, 351 (1970)
43. R. Rikemspoel, Appl. Opt., 3, 351 (1964)
44. R.L. Pecsok and L.D. Shields, "Modern Methods of

Chemical Analysis", Wiley, New York (1968) pp.181

45. B. Chance, Rev. Sci. Inst., 22, 634 (1954)
- B. Chance, "Meth. Enzy. IV", Academic Press, New York, (1957)
46. C. Daniel and F.S. Wood, "Fitting Equations to Data", 2nd ed., John Wiley and Sons, New York, 1980.
47. K.J. Laidler, "Chemical Kinetics", McGraw-Hill, New York (1965)
48. C.J. Collins, Adv. Phys. Org. Chem., 2, 1 (1964)
49. E.S. Swinbourne, "Analysis of Kinetic Data", Thomas Nelson and Sons Ltd., London (1971)
50. A. Albert, W.L.F. Armarego, Adv. Het. Chem., 4, 1 (1964)
51. D.D. Perrin, Adv. Het. Chem., 4, 43 (1964)
52. W.L.F. Armarego, Adv. Het. Chem., 1, 253, (1963)
53. J.P. Guthrie, J. Am. Chem. Soc., 96, 3608 (1974)
54. W.P. Jencks, J. Am. Chem. Soc., 94, 4731 (1972)
55. W.J. Albery, J. Chem. Soc. Faraday Trans. 1, 78, 1579 (1982)

APPENDIX

Table 14. Process (a) Rate Constants for PP+ at 25°C.

pH	k_{obs}, s^{-1}	$\log k_{obs}$
5.15	0.100	-0.999
5.40	0.128	-0.892
5.51	0.135	-0.870
5.65	0.514	-0.813
6.18	0.422	-0.375
6.43	0.722	-0.142
6.63	0.816	-0.0881
7.22	1.42	0.152
7.91	2.40	0.380
8.84	4.17	0.620
9.08	10.70	1.03
9.44	17.7	1.25
9.65	45.6	1.66
10.14	103	2.01

Table 15. Process (b) Rate Constants for PP^+ at 25°C.

pH	$k_{obs} \text{ s}^{-1}$	$\log k_{obs}$
13.85	77.1	1.89
13.55	76.2	1.88
13.35	64.3	1.81
13.1	51.6	1.71
12.85	31.2	1.49
12.35	10.1	1.00
11.85	3.56	0.552
11.35	0.993	-0.00290
10.85	0.257	-0.589
10.3	0.115	-0.941
9.82	0.0413	-1.38
9.01	6.88×10^{-3}	-2.06
8.92	4.20×10^{-3}	-2.38
8.36	1.24×10^{-3}	-2.91
7.14	1.08×10^{-4}	-3.96
6.59	7.16×10^{-5}	-4.14
6.43	5.22×10^{-5}	-4.28

Table 16. Process (c) Rate Constants for PP^+ at $25^\circ C$.

pH	k^{obs}, s^{-1}	$\log k^{obs}$
0.429	0.492	-0.308
0.730	0.696	-0.157
1.13	0.925	-0.0338
1.43	1.008	-0.00377
1.65	0.954	-0.0246
1.95	0.897	-0.0472
2.02	0.945	-0.091 ^a
2.51	0.578	-0.238 ^a
2.90	0.360	-0.443 ^a
3.44	0.179	-0.747 ^a
4.00	0.0817	-1.09 ^a
4.38	0.0491	-1.31 ^a
4.82	0.0607	-1.22 ^a

^aSwinbourne calculated infinity

Table 17. Process (d) Rate Constants for PP+ at 25°C.

pH	k^{obs}, s^{-1}	$\log k^{obs}$
0.429	0.0690	-1.16
0.730	0.0366	-1.44
0.952	0.0240	-1.62
1.43	7.03×10^{-3}	-2.15
1.75	4.13×10^{-3}	-2.38
1.95	1.91×10^{-3}	-2.72
2.47	8.76×10^{-4}	-3.06
3.05	5.32×10^{-4}	-3.27
3.24	4.21×10^{-4}	-3.38
3.78	3.11×10^{-4}	-3.51
4.15	2.24×10^{-4}	-3.65
4.63	1.19×10^{-4}	-3.92
5.42	4.34×10^{-5}	-4.36

Table 18. Ring-Closing of 7-BrPP^+ at 25°C . Fast Process (process (c))

pH	$k_{\text{obs}}, \text{s}^{-1}$	$\log k_{\text{obs}}$
0.429	1.45	0.162
0.730	1.21	0.0831
1.13	0.735	-0.134
1.43	0.471	-0.327
1.77	0.182	-0.740

Table 19. Ring-Closing of 7-BrPP^+ at 25°C . Slow Process (process (d))

pH	k_{obs}	$\log k_{\text{obs}}$
0.429	0.0205	-1.69
0.730	0.0105	-1.98
1.13	0.00610	-2.25

Table 20. Ring-Opening of 7-BrPP⁺ at 25°C.

pH	$k_{\text{obs}}, \text{s}^{-1}$	$\log k_{\text{obs}}$
13.55	28.7	1.46
13.25	31.3	1.49
12.85	33.0	1.52
12.55	27.9	1.45
12.25	19.0	1.28
11.85	9.42	-0.947
11.55	5.39	0.732
10.85	0.908	-0.0419
10.10	0.215	-0.668
9.27	0.0387	-1.41

Table 21. Ring-Closing of 4-MePP+ at 25°C.

pH	$k_{\text{obs}}, \text{s}^{-1}$	$\log k_{\text{obs}}$
0.429	1.86×10^{-2}	-1.73
0.730	1.08×10^{-2}	-1.97
0.952	7.45×10^{-3}	-2.13
1.13	5.52×10^{-3}	-2.26
1.43	3.78×10^{-3}	-2.61

Table 22. Ring-Opening of 4-MePP+ at 25°C.

pH	$k_{\text{obs}}, \text{s}^{-1}$	$\log k_{\text{obs}}$
13.55	2.69	0.430
13.05	0.836	-0.0779
12.55	0.278	-0.557
11.85	0.0502	-1.30
11.55	0.0234	-1.63

Table 23. Ring-Closing of 2,4-diMePP+ at 25°C.

pH	$k^{\text{obs}}, \text{s}^{-1}$	$\log k^{\text{obs}}$
0.429	2.01	0.323
0.730	1.03	0.121
0.952	0.633	-0.198
1.13	0.394	-0.404
1.43	0.218	-0.663
2.11	0.0398	-1.40

Table 24. Ring-Opening of 2,4-diMePP+ at 25°C.

pH	k^{obs}	$\log k^{\text{obs}}$
13.55	0.540	-0.267
13.05	0.156	-0.806
12.55	0.0475	-1.32
11.85	8.09×10^{-3}	-2.09
11.55	3.93×10^{-3}	-2.41

Table 25. Buffer catalysis rate constants for process (c),
cyanoacetate buffers.

pH	[buffer], M	$k_{\text{obs}}, \text{s}^{-1}$
2.57	0.200	0.491
	0.150	0.490
	0.100	0.480
	0.050	0.450
	0.020	0.406
	0.015	0.348
2.16	0.200	0.801
	0.150	0.787
	0.100	0.774
	0.050	0.743
	0.025	0.694
	0.015	0.646
1.73	0.200	0.899
	0.150	0.923
	0.100	0.923
	0.050	0.912
	0.025	0.894
	0.015	0.825

Table 26. Buffer catalysis rate constants for process (c), β -chloropropionate buffers.

pH	[buffer], M	k^{obs} , s ⁻¹
3.78	0.200	0.141
	0.150	0.142
	0.100	0.136
	0.050	0.121
	0.025	0.108
	0.015	0.0975
3.50	0.200	0.199
	0.150	0.194
	0.100	0.189
	0.050	0.185
	0.025	0.173
	0.015	0.162

Table 27. Buffer catalysis rate constants for process (c), chloroacetate buffers.^a

pH	[buffer], M	k_{obs} , s ⁻¹
2.32	0.200	0.708
	0.150	0.698
	0.100	0.701
	0.050	0.681
	0.025	0.638
	0.015	0.594
2.44	0.200	0.632
	0.150	0.632
	0.100	0.621
	0.050	0.599
	0.025	0.560
	0.015	0.526
2.70	0.200	0.478
	0.150	0.470
	0.100	0.457
	0.050	0.438
	0.025	0.413
	0.015	0.370
2.86	0.200	0.392
	0.150	0.392

	0.100	0.381
	0.050	0.361
	0.025	0.327
	0.015	0.300
3.07	0.200	0.299
	0.150	0.290
	0.100	0.280
	0.050	0.258
	0.025	0.235
	0.015	0.185

a. Intercept values were determined by extrapolation from a plot of k^{obs} versus measured pH at 0.005M [buffer].

Table 28. Buffer catalysis rate constants for process (c), formate buffers.

pH	[buffer], M	k_{obs} , s ⁻¹
3.91	0.200	0.145
	0.150	0.136
	0.100	0.124
	0.050	0.107
	0.025	0.0937
	0.015	0.0832
3.25	0.200	0.280
	0.150	0.271
	0.100	0.259
	0.050	0.237
	0.025	0.213
	0.015	0.198
3.72	0.200	0.205
	0.150	0.196
	0.100	0.183
	0.050	0.163
	0.025	0.143
	0.015	0.132

Table 29. Buffer catalysis rate constants for process (c), acetate buffers.

pH	[buffer], M	$k^{\text{obs}}, \text{s}^{-1}$
4.54	0.050	0.123
	0.0375	0.115
	0.025	0.100
	0.0125	0.0852
4.20	0.050	0.139
	0.040	0.139
	0.030	0.127
	0.020	0.111
	0.010	0.0931